November 12, 2013 | vol. 110 | no. 46 | pp. 18341–18736

PNAS

Proceedings of the National Academy of Sciences of the United States of America www.pnas.org

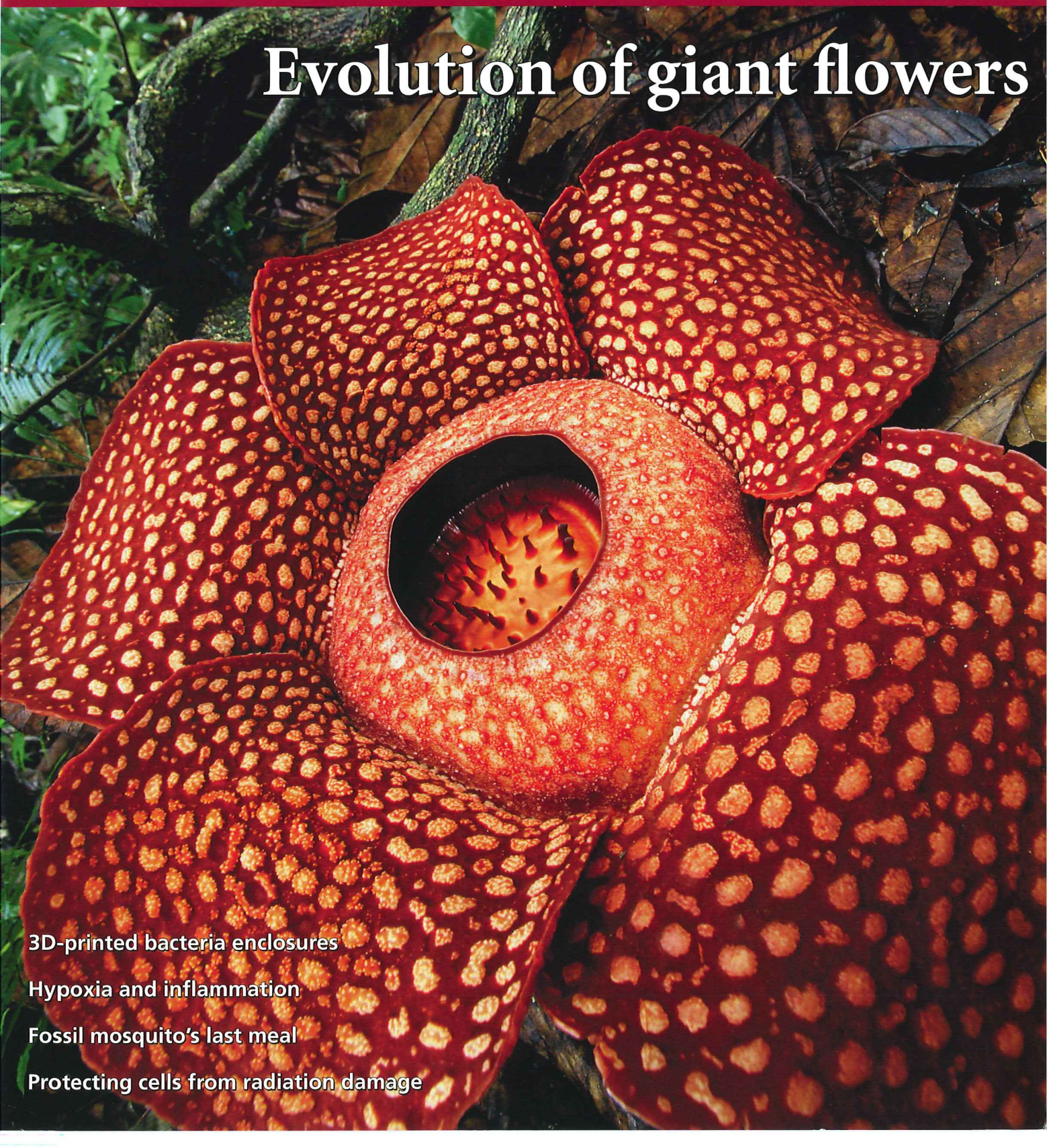

Evolution of giant flowers

3D-printed bacteria enclosures

Hypoxia and inflammation

Fossil mosquito's last meal

Protecting cells from radiation damage

Developmental origins of the world's largest flowers, Rafflesiaceae

Lachezar A. Nikolov[a], Peter K. Endress[b], M. Sugumaran[c], Sawitree Sasirat[d], Suyanee Vessabutr[d], Elena M. Kramer[a], and Charles C. Davis[a,1]

[a]Department of Organismic and Evolutionary Biology, Harvard University Herbaria, Cambridge, MA 02138; [b]Institute of Systematic Botany, University of Zurich, CH-8008 Zurich, Switzerland; [c]Rimba Ilmu Botanic Garden, Institute of Biological Sciences, University of Malaya, 50603 Kuala Lumpur, Malaysia; and [d]Queen Sirikit Botanic Garden, Maerim, Chiang Mai 50180, Thailand

Edited by Peter H. Raven, Missouri Botanical Garden, St. Louis, Missouri, and approved September 25, 2013 (received for review June 2, 2013)

Rafflesiaceae, which produce the world's largest flowers, have captivated the attention of biologists for nearly two centuries. Despite their fame, however, the developmental nature of the floral organs in these giants has remained a mystery. Most members of the family have a large floral chamber defined by a diaphragm. The diaphragm encloses the reproductive organs where pollination by carrion flies occurs. In lieu of a functional genetic system to investigate floral development in these highly specialized holoparasites, we used comparative studies of structure, development, and gene-expression patterns to investigate the homology of their floral organs. Our results surprisingly demonstrate that the otherwise similar floral chambers in two Rafflesiaceae subclades, *Rafflesia* and *Sapria*, are constructed very differently. In *Rafflesia*, the diaphragm is derived from the petal whorl. In contrast, in *Sapria* it is derived from elaboration of a unique ring structure located between the perianth and the stamen whorl, which, although developed to varying degrees among the genera, appears to be a synapomorphy of the Rafflesiaceae. Thus, the characteristic features that define the floral chamber in these closely related genera are not homologous. These differences refute the prevailing hypothesis that similarities between *Sapria* and *Rafflesia* are ancestral in the family. Instead, our data indicate that *Rafflesia*-like and *Sapria*-like floral chambers represent two distinct derivations of this morphology. The developmental repatterning we identified in *Rafflesia*, in particular, may have provided architectural reinforcement, which permitted the explosive growth in floral diameter that has arisen secondarily within this subclade.

ABC model | comparative gene expression | evo-devo | gigantism | parasitic plants

It has been long recognized that parasitism elicits fundamental changes to an organism's body plan (1, 2). Similarly, extreme changes in body size can result in dramatic morphological modifications, which in some cases rise to the level of what we term "novelty'" (3–5). Either of these circumstances can pose challenges to understanding structural homology. One lineage that exhibits both complications is the holoparasitic plant family Rafflesiaceae, which produces the world's largest flowers. Despite their fame, however, the developmental basis of these giants has remained a mystery for nearly two centuries (6, 7). Their floral structure, in particular, is highly modified with respect to most angiosperms, so much so that confusion over their flowers has resulted in Rafflesiaceae-centric terminology to evade statements of homology. This uncertainty has obscured our understanding of their evolutionary origin, which until recently has been unknown (8–10).

Most members of the family possess a large, bowl-shaped floral chamber [sometimes referred to as a chamber blossom by pollination biologists (11, 12)]. The floor and walls of this chamber are formed by a perianth tube and the roof is defined by an organ called the diaphragm (Fig. 1 and Fig. S1 *A* and *C–E*). The opening of the diaphragm serves as the entrance for carrion fly pollinators (13, 14). The chamber is in turn surrounded by a series of attractive sterile organs, termed perianth lobes (Fig. 1 and Fig. S1 *A*, *C–E*, and *G–K*). The central part of the chamber accommodates the central column, which expands distally to form a disk bearing the reproductive organs (Fig. 1 and Fig. S1). Like their closest relatives, Euphorbiaceae, the flowers of Rafflesiaceae are typically unisexual (9). In female flowers, a stigmatic belt forms around the underside of the reproductive disk (13); in male flowers this is where the stamens are borne.

Each of the three genera of Rafflesiaceae produces flowers that vary on this general theme. *Rafflesia* and *Sapria* have a similar floral architecture, but differ in their perianths: *Rafflesia* has one whorl of five perianth lobes (Fig. 1*A*) and *Sapria* has two whorls (Fig. 1*C*), each with five similar lobes. Because of the striking similarity in floral morphology of these two genera, which represent the bulk of species diversity in the family, their floral chambers have been assumed to have originated once in the common ancestor of Rafflesiaceae (15) (Fig. 1). The exception is the species-poor clade *Rhizanthes*, which lacks the floral chamber found in most Rafflesiaceae (16) (Fig. 1*B*). *Rhizanthes* has 16 similar perianth lobes and does not form a diaphragm or chamber closure as in *Rafflesia* and *Sapria*. The perianth lobes in *Rhizanthes* also differ considerably in morphology: they are much narrower, have elaborate hairy "pads," and terminate with distinct tail-like appendages (Fig. 1 and Fig. S1 *G–K*). Based on its more nested phylogenetic placement within the family, it has been assumed that the morphology of *Rhizanthes* is uniquely derived (15). The unusual floral organs of

Significance

Rafflesiaceae produce the world's largest flowers, but the developmental nature of their floral organs has remained a mystery. Most members of the family have a large floral chamber, which encloses their reproductive organs. We used comparative studies of development and gene-expression patterns to investigate the homology of their floral organs. Our results demonstrate that the similar floral chambers in two Rafflesiaceae subclades are constructed very differently. Thus, the characteristic features that define the floral chamber in these closely related clades are not homologous. Instead, these data indicate that similar floral chambers represent two distinct derivations of this morphology, which may have contributed to the explosive growth in floral diameter that arose secondarily within one subclade, *Rafflesia*.

Author contributions: L.A.N., P.K.E., E.M.K., and C.C.D. designed research; L.A.N., M.S., S.S., and S.V. conducted field collections; L.A.N. performed research; L.A.N., P.K.E., E.M.K., and C.C.D. analyzed data; L.A.N., P.K.E., E.M.K., and C.C.D. wrote the paper.

The authors declare no conflict of interest.

This article is a PNAS Direct Submission.

Data deposition: The sequence reported in this paper has been deposited in the GenBank database, http://www.ncbi.nlm.nih.gov/genbank/ (accession nos. KF730013–KF730100).

[1]To whom correspondence should be addressed. E-mail: cdavis@oeb.harvard.edu.

This article contains supporting information online at www.pnas.org/lookup/suppl/doi:10.1073/pnas.1310356110/-/DCSupplemental.

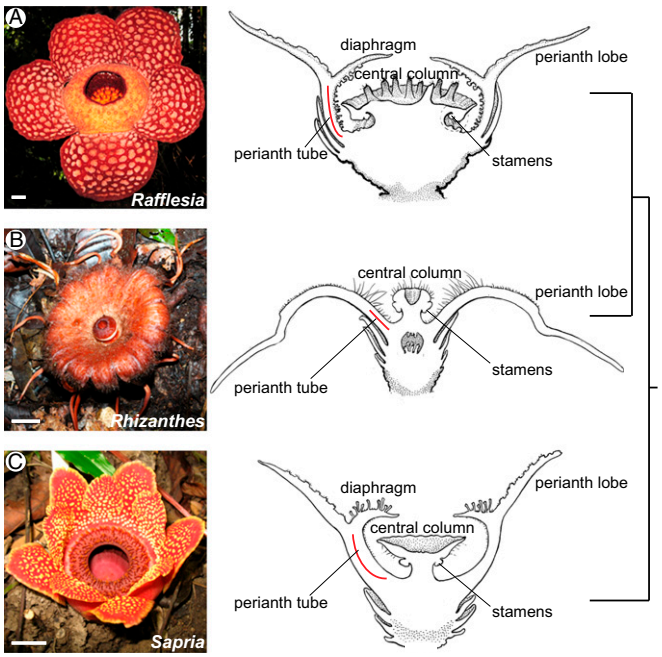

Fig. 1. Gross morphology, longitudinal sections, and accepted phylogenetic relationships of Rafflesiaceae. *Rafflesia* (*A*) and *Sapria* (*C*) exhibit floral chambers, defined by a diaphragm, where the central reproductive column resides. The central column of *Rhizanthes* (*B*) is exposed because no floral chamber is formed. (Scale bars, ~2 cm.) Photo credits: (*A*) D. Boufford, (*B*) C.C. D., (*C*) L.A.N.

Rafflesiaceae pose a serious challenge to understanding their homology and, thus, their evolution.

Like so many branches in the Tree of Life, Rafflesiaceae are not amenable to traditional genetic manipulation, even less so than most plants. These holoparasites grow vegetatively inside their hosts and lack obvious leaves, stems, and roots. The plants have never been successfully propagated, and do not occur outside of their host range in the rainforests of Southeast Asia. Under these circumstances, only multiple independent lines of inquiry can be used to understand the floral structure and evolution of these charismatic plants, including comparative structural, developmental, and gene-expression data. In terms of this last source of data, the ABC model of floral development provides a predictive framework for understanding the identities of the floral organs of Rafflesiaceae (17, 18). The model involves three gene activities: *A* activity alone specifies sepal identity, *A*+*B* define petals, *B*+*C* confer stamen identity, and *C* determines carpel identity. Although it has been recognized that some aspects of the ABC model do not apply to all angiosperms (19), the specification of petal, stamen, and carpel identity by B- and C-class genes is generally conserved in core eudicots (20). In general, great care must be taken when using gene-expression patterns as criteria for establishing homology (21); however, when such correlative data are combined with explicit phylogenetic and developmental data, this approach has been shown to provide critical insights into organ homology (e.g., ref. 22). Along these lines, we cloned homologs of the ABC class genes, which largely belong to the pan-eukaryotic MADS-box (after the four founding members of the family: *MCM1*, *AGAMOUS*, *DEFICIENS*, and *SRF*) gene family (20), from Rafflesiaceae and studied their expression in different floral organs. We complemented these analyses with an investigation of floral organ initiation and development in all three genera in the family.

Our analyses surprisingly demonstrate that the otherwise similar floral chambers in *Rafflesia* and *Sapria* are constructed very differently. In *Rafflesia*, the diaphragm is derived from the petal whorl, whereas normal petals are absent. In contrast, in *Sapria* the diaphragm is derived from elaboration of a unique ring structure located between the perianth and the stamen whorl. This structure is analogous to sterile organs that have been independently derived in other angiosperms, such as the trumpet in daffodils (23) and the corona in passionflowers (24). The structure is not present in the closest relatives of Rafflesiaceae, and is elaborated to varying degrees in all three genera of Rafflesiaceae. Thus, the structures that define these similar floral chambers are not homologous. In *Rhizanthes*, which lacks a diaphragm, a derivative of the ring primordium appears to be adnate to the perianth. The development of this organ is more similar to that of *Sapria*, and is likely a shared symplesiomorphic feature in these two genera. These differences in construction among the three genera refute the simplistic scenario in which the similarities between *Sapria* and *Rafflesia* are interpreted as ancestral in the family.

Results

Cloning of MADS-Box Transcription Factors in Rafflesiaceae. We cloned 28 MADS intervening keratin-like and C-terminal (MIKC) MADS-box genes from Rafflesiaceae and 62 MIKC MADS-box genes from representatives of their closest relatives: Peraceae, Euphorbiaceae, and Phyllanthaceae (Fig. S2*A*) (9, 10). We initially confirmed gene orthology using phylogenetic reconstruction from a broad sample of MADS-box genes, followed by more focused taxon-rich analyses within particular MADS-box subfamilies (Fig. S2 *B–F*; see *Supporting Information* for details). Single copies of the B-class lineages *PISTILLATA* (*PI*) and *APETALA3* (*AP3*), and the C/D-class genes *AGAMOUS* (*AG*) and *SEEDSTICK* (*STK*), were recovered from *Rafflesia* (*RfPI, RfTM6, RfSTK*, and *RfAG*), *Rhizanthes* (*RhPI, RhTM6, RhSTK*, and *RhAG*), and *Sapria* (*SapPI, SapTM6*, and *SapAG*) (Fig. S2*A*). Our degenerate cloning approach was successful in recovering members of several other MADS-box subfamilies (e.g., single homologs of *SEPALLATA1*, *FRUITFUL*, *AGL3, AGL15*, and *SVP* in Rafflesiaceae, one copy of *AGL24* in *Rafflesia*, and duplicate copies of *AGL24* in *Rhizanthes*). As additional verification of gene identity, all homologs possessed the expected C-terminal motifs characteristic of their respective gene lineages (Fig. S3). We did not detect duplicate copies in the floral identity MADS-box repertoire of Rafflesiaceae, even for representatives of the core eudicot hexaploidization event, such as *euAP3* or *PLENA* (25, 26). Thus, these paralogs have either been lost from the genome or are expressed at negligibly low levels. However, species-specific duplications were detected in a number of outgroup taxa. We identified recent duplicates or alleles of *PI* from *Clutia* and *Pera* (Peraceae) (Fig. S2*B*); *euAP3* is duplicated in *Garcia* (Euphorbiaceae); and *TM6* is present in two copies in *Clutia* (Peraceae) and *Jatropha* (Euphorbiaceae) (Fig. S2*C*). *AG* is duplicated in all outgroup taxa, although most of these duplications appear to be species-specific (Fig. S2*D*).

Comparative Organ Identity Gene Expression. We sampled all major organs and regions of Rafflesiaceae flowers for expression of organ identity genes (Fig. S4). Our initial survey showed that most of the MADS-box homologs we identified are broadly expressed across individual floral organs (Fig. S5 *A–C*). Two notable exceptions were Rafflesiaceae *PI* and *AG* homologs, which are differentially expressed in different floral organs (Fig. 2). We therefore focused our analysis on these loci because the B- and C-class genes are the most conservative elements of the floral organ identity module in core eudicots (17). Thus, they have greater predictive power for interpreting floral organ homology.

RfPI is strongly expressed in the diaphragm and stamens with detectable signal seen in the perianth tube (Fig. 2*A*). *RfAG* expression is restricted to the central column, including the stamens

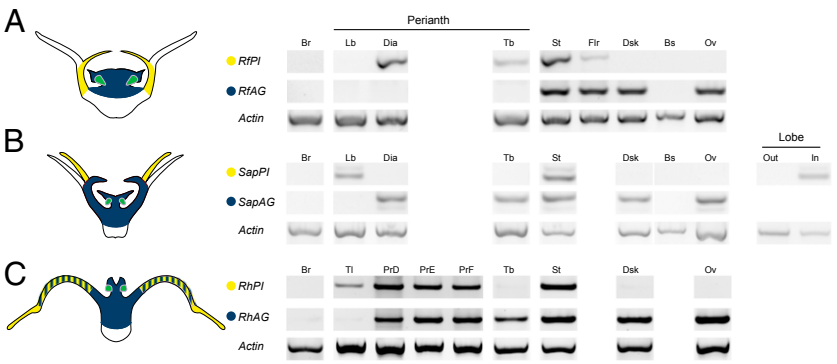

Fig. 2. *PISTILLATA* (*PI*, B-class) and *AGAMOUS* (*AG*, C-class) gene expression in Rafflesiaceae flowers. (*A*) *Rafflesia PI* and *AG* homologs abbreviated *RfPI* and *RfAG*. (*B*) *Sapria*, *SapPI*, and *SapAG;* In, inner perianth lobes; Out, outer perianth lobes. (*C*) *Rhizanthes*, *RhPI,* and *RhAG*; PrD, -E, and -F are perianth regions indicated in Fig. S6. Tl, tails. Actin is used as a concentration control. Abbreviations of dissected floral organs are as follows: Br, bracts; Bs, base of the flower; Dia, diaphragm; Dsk, disk; Flr, floor of the floral chamber; Lb, perianth lobes; Ov, ovary; St, stamens; Tb, perianth tube, (see Fig. S4 for the position of these regions). Gene-expression summaries illustrated to the left are shaded as follows: *PI* expression in yellow, *AG* expression in dark blue. The overlap of *PI* and *AG* in stamens is shown in green and in the proximal lobes of *Rhizanthes* with blue and yellow hatching.

in male flowers and the inferior ovary of female flowers. The expression of *Sapria PI* is limited to the inner perianth whorl (Fig. 2*B*). A signal is also seen in the stamens of male flowers. *SapAG* exhibits a broad pattern of expression, and is detected in the diaphragm, perianth tube, throughout the central disk, including the stamens of male flowers and the ovary of female flowers. Expression studies in *Rhizanthes* (Fig. 2*C*) are complicated by the complex nature of the perianth (see below). *RhPI* is expressed throughout the perianth lobes, including the tails, and stamens of male flowers. *RhAG* is broadly expressed throughout the floral organs with the exception of the tails. In addition to the stamens, *RhAG* expression overlaps with *RhPI* expression in the proximal portion of the perianth lobes.

We also examined B- and C-class gene expression in the close relative of Rafflesiaceae, *Clutia* (Peraceae), which bears more typical flowers. *Clutia* has unisexual flowers with both sepals and petals (Fig. S5*D*). In female flowers, the carpels are surrounded by stamen-derived nectaries borne opposite the sepals (27). We examined expression in dissected sepals, petals, and carpels from several female flowers. As expected, the B-class gene *CluPI* is expressed only in the petals. *CluAP3* and *CluTM6* are expressed throughout the flower, with *CluTM6* most strongly expressed in the petals. *CluAG* is expressed in the carpels. Weak expression of *CluAG* was also detected in the sepals but this is likely a result of cross-contamination with the nectary, which is closely associated with the base of the sepals. Given that the nectaries are likely stamen-derived (27), they may express C-class genes, but these organs could not be reliably dissected.

Developmental Morphology of Rafflesiaceae. We performed extensive sampling of developmental stages from all three genera of Rafflesiaceae to further understand floral organ identity. In *Rafflesia*, the five perianth lobes appear sequentially in a spiral (Fig. 3*A*). Closely following the appearance of the perianth lobes, but preceding the appearance of the stamens, the diaphragm in *Rafflesia* arises as a ring that extends toward the center of the apex (Fig. 3 *A* and *B*). The perianth lobes and the diaphragm are raised above the apex by intercalary growth, which forms the perianth tube. Stamens are initiated on the flanks of the broad, convex floral apex (Fig. 3 *C* and *D*). At about the same time, an additional ring structure appears just outside of the stamens, which seems to be derived from the floor of the chamber (Fig. 3 *C* and *D*). Although at an early stage both the stamens and this ring are of comparable size (Fig. S6*A*), the ring does not expand much further and becomes comparatively inconspicuous. The ring is present at the base of the disk in advanced floral buds and in open flowers (Fig. S1 *A* and *B*).

In *Sapria*, the perianth lobes appear nearly simultaneously as two alternating whorls (Fig. 3*E*). The perianth lobes of the outer whorl are acute at the apex and broad at the base near the level of attachment (Fig. 3*F*). In contrast, lobes of the inner whorl are rounded at the apex and narrower at the base (Fig. 3*G*). Although the two whorls differ conspicuously at this early stage, these differences diminish as development proceeds to anthesis (Fig. 1*C*). In contrast to *Rafflesia*, the diaphragm in *Sapria* appears later in development, at the same time or shortly after the stamens appear, from a ring primordium outside of the stamen whorl (Fig. 3*G*). Intercalary growth below the diaphragm lifts the diaphragm together with the two whorls of perianth lobes forming the perianth tube (Fig. 3*H*).

The 16 perianth lobes of *Rhizanthes* appear in two whorls of eight lobes each (Fig. 3*I*). The lobes form nearly simultaneously in a circle on the flanks of a broad floral apex and then grow in horizontal direction toward each other (Figs. 3 *J* and *K*). Their round tips touch, bend downward, and continue elongating toward the floral apex, which is slightly concave at this stage (Fig. 3*K*). The lobes' descending portions, which correspond to the tails, are tightly appressed to each other in bud (Fig. 4*C* and Fig. S1*J*). At this later stage, the stamen whorl also appears and, concomitantly, a ring structure arises outside the stamen whorl (Fig. 3*J*). The ring becomes congenitally fused to, and elongates with, the perianth lobes as they grow (Fig. S6 *B–F*), ultimately forming the pads at the base of each perianth lobe (Fig. S1 *H–K*). The adnation between the ring and the perianth is discernible histologically (Fig. S6 *B–F*).

Additional Floral Morphological Landmarks in Rafflesiaceae. Finally, we made a detailed study of gross morphological landmarks in all three genera of Rafflesiaceae. In *Rafflesia*, the reproductive column is notable for the presence of alternating longitudinal grooves and ridges that begin at the ring and extend to the base of the disk (Fig. 4*A*). The grooves accommodate individual anthers in male flowers but are also present in female flowers, which have a highly reduced stamen whorl. Similar grooves and ridges are found on the inner surface of the perianth tube in *Sapria*, and here they extend from the undersurface of the diaphragm to the base of the central column (Fig. 4*B* and Fig. S1 *D* and *E*). Finally, the perianth tube of *Rhizanthes* exhibits shallow grooves and ridges demarcated by dark striations, from the attachment of the central column to the beginning of the perianth lobes, which similarly alternate with the stamens in male flowers and staminodia in female flowers (Fig. 4*C*).

Another peculiar morphological feature in *Rafflesia* and *Sapria* is the presence of a series of multicellular, vascularized, branched structures called ramenta. In *Rafflesia*, the ramenta line the inner surface of the perianth tube and extend from outside the ring at the base of the central column to the undersurface of the diaphragm (Fig. 4*A* and Fig. S1*A*). In contrast, the ramenta in *Sapria* are restricted to the upper surface of the diaphragm and are absent from the inside of the chamber (Fig. 4*B* and Fig. S1 *C–F*). Ramenta, similar to those observed in *Rafflesia* and *Sapria*, are absent in *Rhizanthes*, which instead exhibits a variety of unicellular trichomes covering the adaxial side of the perianth (Fig. 4*C* and Fig. S1 *G–K*).

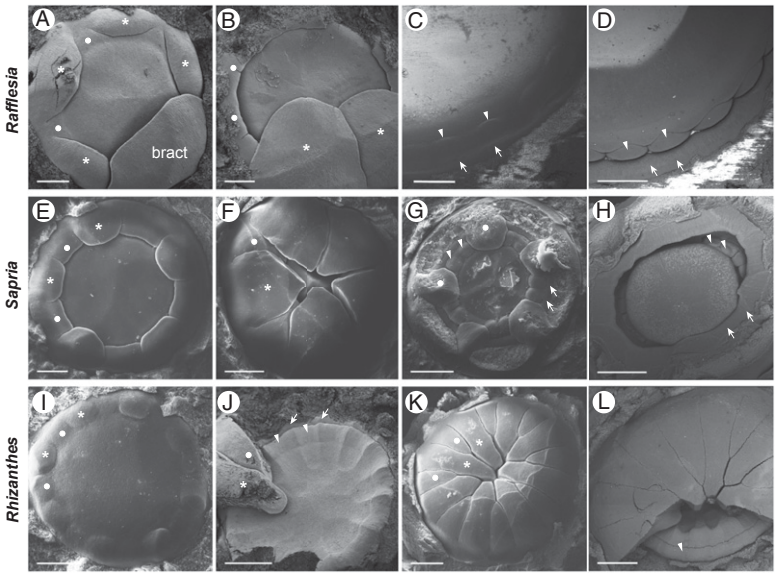

Fig. 3. Floral development in *Rafflesia* (*A–D*), *Sapria* (*E–H*), and *Rhizanthes* (*I–L*). (*A*) Spiral initiation sequence of the perianth lobes (asterisks) of *Rafflesia*, with all but one bract removed; the diaphragm appears as a ring (dots). (*B*) The diaphragm (dots) extends horizontally toward the center of the flower; all but the last two perianth lobes (asterisks) removed. (*C*) Stamen (arrowheads) and (inner) ring (arrows) initiation. (*D*) Later stage of stamen (arrowheads) and ring (arrows) development; the diaphragm has been removed but is apparent as the darker band around the lighter center. (*E*) Two whorls of perianth lobes are initiated at alternate positions in *Sapria* (asterisks and dots). (*F*) The outer whorl perianth lobes (pointed tips, asterisk) cover the inner whorl (dot). (*G*) Five clawed inner perianth lobes (dots) and the initiation of the stamen whorl (arrowheads) and the (inner) ring (arrows); five outer perianth lobes removed. (*H*) The diaphragm (arrows) is lifted above the stamens (arrowheads) by intercalary growth. (*I*) Appearance of perianth lobes in *Rhizanthes* at the flanks of a broad floral apex; asterisks and dots indicate alternating perianth organs. (*J*) Initiation of stamens (arrowheads) and a ring outside of the stamens (arrows); all but two perianth lobes removed (asterisk and dot). (*K*) Two whorls of 8+8 alternating lobes (asterisks and dots). (*L*) A more advanced stage of stamen development (arrowhead) and the formation of a concave floral apex. (Scale bars: 500 μm in *A–C*, *E*, *I*, *J*, *L*; 1 mm in *D*, *F–H*, *K*.)

Discussion

Integrating Molecular, Developmental, and Morphological Data to Elucidate Floral Organ Homologies in Rafflesiaceae. In all three genera of Rafflesiaceae, the reproductive column expresses *AG* homologs with *PI* homologs restricted to the stamens. This similarity in expression is consistent with the conserved structure of the column, which is likely homologous across the family. The perianth organs of *Rafflesia*, *Sapria*, and *Rhizanthes*, however, exhibit very distinct patterns of organ identity gene expression, despite their positional similarity. In *Rafflesia*, the diaphragm and perianth tube express the B-class gene *RfPI*, whereas in *Sapria SapPI* is restricted to the inner perianth lobes (Fig. 2). The broad expression found in other Rafflesiaceae B-class genes, namely the *TM6* homologs, is not significant because PI and TM6 proteins typically function as obligate heterodimers (28). Restricted expression of *PI*, therefore, limits the breadth of B-class gene function to the diaphragm and perianth tube in *Rafflesia* and to the inner perianth lobes in *Sapria*. B-class function specifies petals in model core eudicots (17) and, as expected, *CluPI* expression is also specific to the petals in the close relative of Rafflesiaceae, *Clutia*. These observations suggest that the diaphragm in *Rafflesia* and the inner perianth lobes in *Sapria* possess petal identity. Gene expression in *Rhizanthes* more closely resembles *Sapria* than *Rafflesia* in that *RhAG* expression is expanded to include the perianth tube and even portions of the perianth lobes, but not the distal-most region of the lobes that form the tails. Although *RhAG* expression appears to overlap with that of *RhPI* in the more proximal pads of the perianth lobes, we hypothesize that this overlap likely reflects *RhAG* expression in the ring-derived adaxial pads, whereas *RhPI* is expressed in the abaxial layers of the perianth proper (Fig. 2 and Fig. S6*D*). This interpretation indicates a likely homology between the ring-derived diaphragm of *Sapria* and the ring-derived series of pads of *Rhizanthes*.

Differential gene expression among the genera of Rafflesiaceae, particularly between *Sapria* and *Rafflesia*, which look superficially similar, can be explained in two ways. First, they could reflect dramatic shifts in gene expression that are independent of the homology of the structures themselves (21). This is the case for the sepal-derived and highly modified perianth of *Aristolochia*, which appears to express B-class genes (29). Second, they could represent the actual identity, and thus homology, of the organs (30, 31). To determine which of these two scenarios is more plausible, we examined the initiation and elaboration of the floral organs in Rafflesiaceae. In all three genera, organ initiation is organized into two waves. The perianth organs appear first, including the perianth lobes and diaphragm in *Rafflesia* and the two whorls of perianth lobes in *Sapria* and *Rhizanthes*. Second, we see initiation of the stamens along with an adjacent ring primordium between the perianth and the stamen whorl that does not correspond to any canonical floral whorl. This ring remains a relatively minor feature in *Rafflesia*. In contrast, in *Sapria* the ring structure becomes prominent in giving rise to the diaphragm; in *Rhizanthes* it forms the series of pads on the perianth lobes. The distinct fates and positions of the ring derivatives in *Rafflesia* versus *Sapria*/*Rhizanthes* reflect a combination of differential elaboration of the structures themselves (less in *Rafflesia*, more in *Sapria* and *Rhizanthes*). In *Rafflesia*, intercalary expansion occurs between the ring and the perianth whorl, whereas in *Sapria* it occurs between the ring and the base of the column. In *Rhizanthes*, some intercalary growth also occurs between the ring and the base of the column, but the deep lobing of the perianth makes identification of intercalary growth in this case more difficult to interpret.

These developmental patterns correlate perfectly with our gene-expression data: early arising inner perianth organs (i.e., the diaphragm in *Rafflesia* and the inner lobes of *Sapria*) express *PI* homologs alone but ring-derived structures express *AG* homologs (the chamber floor in *Rafflesia*, diaphragm in *Sapria*, and series of pads of *Rhizanthes*). Further evidence for this correspondence comes from our assessment of gross morphology: grooves and ridges are always present between the ring-derived structures and the base of the reproductive column; in *Rafflesia* and *Sapria* ramenta line the region between the ring and the inner perianth organs. The positions of these key floral landmarks—ridges/grooves and ramenta—are most easily explained by the hypothesis that intercalary growth in different regions gave rise to the similar floral chambers in *Rafflesia* and *Sapria*. In terms of our identification of the *Rafflesia* diaphragm as the petal whorl, it is interesting to note that considerable variation in diaphragm morphology is observed in many species of *Rafflesia*. Some have distinctly lobed diaphragms, and others have reduced diaphragms that form a small shelf at the chamber opening (32). Elucidating the developmental basis of this variation may shed light on the modification of this floral organ.

All three sources of evidence—gene expression, development, and morphological landmarks—indicate that the diaphragm of *Rafflesia* is derived from the petal whorl, but the diaphragm of

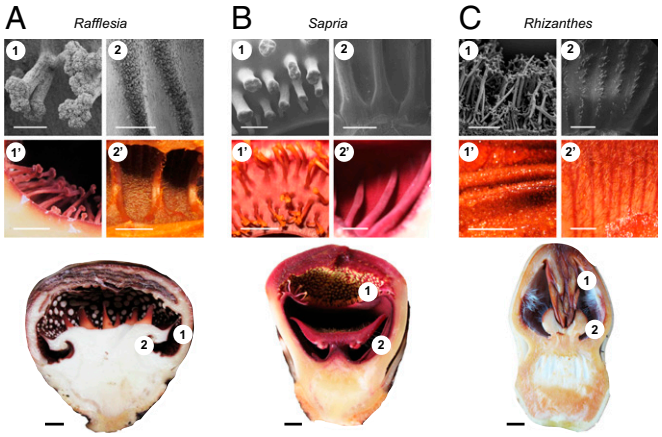

Fig. 4. Gross floral morphological landmarks in *Rafflesia* (*A*), *Sapria* (*B*), and *Rhizanthes* (*C*). The positions of the ramenta (in *Rafflesia* and *Sapria*) or trichomes (in *Rhizanthes*) (1 and 1′) and ridges/grooves (2 and 2′) across the three genera are compared using SEM (1 and 2) and light photography (1′ and 2′). [Scale bars: SEM micrographs, 1 mm (except C1, which equals 500 μm); photographs, 5 mm.] Circles numbered 1 and 2 in the bottom photographs indicate the position of these key morphological landmarks in advanced floral buds. (Scale bars, 1 cm.)

Sapria is derived from the unique ring structure. This conclusion suggests that diaphragm formation is not homologous in *Rafflesia* and *Sapria*. It appears that in *Rafflesia*, the chamber is primarily formed via expansion of the congenitally fused sepal and petal bases, which constitute the perianth tube. In contrast, in *Sapria*, the sepal and petal whorls develop as free lobes that do not contribute to the formation of the floral chamber, which instead forms by elaboration of the ring structure. The modifications seen in *Rhizanthes* are more complex and involve fusion of the ring to the perianth as well as deep dissection of this compound structure. Regardless, in all three genera the structures derived from the ring primordium express *AG* homologs, which is not surprising because they originate in close proximity to the base of the reproductive column. In this sense, the ring of *Rafflesia*, the diaphragm of *Sapria*, and the series of pads of *Rhizanthes* bear parallels to peculiar outgrowths, called coronas, seen in divergent angiosperm clades, including the radial filaments (commonly termed "crown of thorns") in passionflowers (24) and the trumpet of daffodils (23). In these cases, the coronas are also initiated late in development, after significant elaboration of the other floral organs, and they express *AG* homologs, despite the fact that they are sterile organs.

Evolution of the Floral Chamber in Rafflesiaceae. Our results refute the simplistic scenario of floral evolution proposed for Rafflesiaceae, in which the floral chamber in *Rafflesia* and *Sapria* is thought to represent the ancestral condition within the family, which was then lost in *Rhizanthes* (15). Instead, our data suggest that the floral chambers in *Rafflesia* and *Sapria* are constructed differently and the involvement of the petal whorl is a *Rafflesia*-specific invention. Given the evolutionary and phenotypic distance between Rafflesiaceae and its common ancestor with Euphorbiaceae (~95 My) (15) and the widely accepted fact that parasitism can lead to drastic changes that confound assessment of homology (2, 8, 33), outgroup comparisons with Euphorbiaceae are problematic for understanding floral evolution in Rafflesiaceae.

If we instead focus on Rafflesiaceae, one model is that the closed floral chambers characteristic of the family have arisen independently in *Rafflesia* and *Sapria*, perhaps because of similar selective pressures imposed by fly pollinators (Fig. S7*A*). In this case, the common ancestor of Rafflesiaceae lacked an organized floral chamber and this ancestral condition was retained in *Rhizanthes*. A similar example has been documented in two related groups, *Aristolochia* and *Hydnora*, which have evolved floral chambers with different construction. In *Hydnora*, the roof of the chamber is formed by the stamens; in *Aristolochia* it is formed by the perianth (29, 34). A second model would be that the common ancestor of Rafflesiaceae possessed a floral chamber similar to that in *Sapria* [i.e., derived from expansion between the ring and the column (Fig. S7*B*)]. This floral chamber was then lost along the branch leading to *Rhizanthes* and remodeled along the branch leading to *Rafflesia*, such that the diaphragm was derived from the petal whorl. Under the second model there would have been relatively little change in the gross morphology of these floral chambers. Despite this superficial similarity, however, the underlying development of the *Rafflesia* and *Sapria*-like floral chambers would have been completely repatterned. Variation in the timing of these changes can also produce a third model (e.g., Fig. S7*C*).

This second model might seem unlikely, especially because the fly pollinators that visit these plants appear to be shared between the three Rafflesiaceae genera (13–16). However, such changes are not without precedent and have been explained by developmental system drift (35). This is a process by which characters that are thought to be homologous have diverged in their morphogenetic or gene regulatory underpinnings. For example, developmental system drift underlies the conservation of the segmented body plan in insects, which nonetheless exhibits variability in the underlying mechanisms of segmentation (36, 37). Detailed investigation of this phenomenon requires functional comparison between two species with the same body plan to understand changes in the underlying molecular machinery (38), and as such it is not feasible in Rafflesiaceae. Moreover, although such studies may illuminate important mechanistic features of the developmental system, they cannot explain the underlying reasons for such a striking change in development.

So why then has *Rafflesia*, which contains the largest of all flowers (*Rafflesia arnoldii* R.Br., 1 m in diameter), undergone such profound developmental repatterning? The developmental genetic mechanisms that permit flower size to increase rapidly remain unknown for this or any other lineage (12). Interestingly, although the early ancestors of Rafflesiaceae exhibited a dramatic increase in floral size (9), it appears that within the family, rates of floral size evolution were further elevated in *Rafflesia* (39). One potential explanation for this pattern is that the change we have posited for *Rafflesia* floral development could have further reduced constraints on floral diameter and permitted its additional burst in gigantism. Several factors, including an earlier shift in the developmental timing of diaphragm initiation, the effective reduction in the perianth lobes, and the architectural remodeling of the chamber itself, could have contributed to the stabilization of these enormous flowers. Support for this hypothesis comes from the occurrence of lobed (imperfectly formed) diaphragms in *Rafflesia*, which are restricted to species of small size [e.g., *Rafflesia lobata* Barcelona & Pelser (32)]. Further investigation within *Rafflesia* will help to better address this question, but overall, our study highlights the surprising and dynamic nature of morphological evolution among the "greatest prodigy of the vegetable kingdom" (6). In particular, the study underscores the degree to which seemingly similar morphologies can be fundamentally remodeled among closely related species.

Materials and Methods

Plant Material. Buds of *Rafflesia tuan-mudae* Becc. and *Rafflesia cantleyi* Solms-Laubach in different developmental stages were collected in Gunung Puey, Sarawak, and in Ulu Geroh, Peninsular Malaysia, respectively. *Sapria himalayana* Griffith was collected at Queen Sirikit Botanic Garden, Chiang Mai, Thailand. *Rhizanthes lowii* (Becc.) Harms was collected near Kampung

Giam, Sarawak. Vouchers are deposited at the Harvard University Herbaria (A). The historical collection of *Rafflesia patma* Blume by A. Ernst is housed at the Botanical Institutes of the University of Zurich (Z). *Clutia* sp. and *Pera bumeliifolia* Griseb. were collected from the University of California Davis Botanical Conservatory and Fairchild Tropical Botanic Garden, respectively, and vouchers are deposited at the University of California at Davis herbarium (DAV) and Fairchild Tropical Botanic Garden herbarium (FTG). *Dalechampia* sp., *Breynia* sp., *Acalypha* sp., *Garcia* sp., *Monadenium* sp., and *Jatropha* sp. were obtained from living material at the University of Connecticut greenhouse and vouchers are deposited at the University of Connecticut herbarium (CONN).

RNA Isolation, cDNA Synthesis, and Cloning of MADS-Box Genes. Floral material from both male and female buds of different sizes (diameter of *Rafflesia* floral buds ranging from 5 to 25 cm; *Sapria* from 3 to 15 cm; and *Rhizanthes* from 2 to 13 cm) was dissected and flash-frozen in the field, then kept at −80 °C until RNA isolation. Total RNA was extracted from 0.1- to 0.5-g tissue using Plant RNA Reagent (Invitrogen) following the manufacturer's recommendations. DNA contamination was eliminated after incubation with TURBO-DNase (Ambion) for 2 h and total DNased RNA were used for cDNA synthesis using polyT primer (40) with SuperScript RT II (Invitrogen). Degenerate primer approach was used to clone MADS-box genes from Rafflesiaceae and outgroups as previously described (for A-class products, see ref. 40; for B- and C-class products, see ref. 41). All sequences were recovered independently from a minimum of three clones, but typically from more than 50 clones (GenBank accession nos. KF730013–KF730100). Sequences were examined and edited manually in Geneious (Geneious).

RT-PCRs. The floral buds were dissected into several nonoverlapping regions (Fig. S4). One to 5 μg of DNased, organ-specific RNA from the same regions of at least three floral buds (biological replicates) were used separately for cDNA synthesis as described above. Gene-specific primers (Table S2) spanning an intron were used in a PCR with one-tenth dilution of cDNA with 55 °C annealing, 15-s elongation time, and 26 cycles. Products were separated on 1.5–2% agarose gels. Actin amplification was used as an internal control.

ACKNOWLEDGMENTS. We thank K. Bomblies, D. Boufford, C. Extavour, W. Friedman, D. Haig, A. Knoll, S. Mathews, B. Tomlinson, and members of the C.C.D., E.M.K., and W. Friedman laboratories for valuable comments; S.-Y. Wong and members of the S.-Y.Wong laboratory, M. Wong, R. Pongsattayapipat, and the staff at Queen Sirikit Botanic Garden, S. Sari, and B. Insan for field support; the University of California, Davis conservatory and the University of Connecticut greenhouse for living plant material; M. Matthews for help with microtome sectioning; R. Hellmiss for help with the graphics; B. Angell for the illustrations; and C.-C. Wu for providing the initial MADS box alignments and related information. Imaging support was provided by the Center for Microscopy and Image Analysis at the University of Zurich and the Center for Nanoscale Systems at Harvard University. This research was supported by National Science Foundation Assembling the Tree of Life Grant DEB-0622764 (to C.C.D.), and National Science Foundation Grant DEB-1120243 (to C.C.D. and E.M.K.).

1. Bush AO, Fernandez JC, Esch GW, Seed JR (2001) *Parasitism: The Diversity and Ecology of Animal Parasites* (Cambridge Univ Press, Cambridge, UK).
2. Kuijt J (1969) *The Biology of Parasitic Flowering Plants* (Univ of California Press, Berkeley, CA).
3. Emlen DJ, Nijhout HF (2000) The development and evolution of exaggerated morphologies in insects. *Annu Rev Entomol* 45:661–708.
4. Sander PM, et al. (2011) Biology of the sauropod dinosaurs: The evolution of gigantism. *Biol Rev Camb Philos Soc* 86(1):117–155.
5. Hanken J, Wake DB (1993) Miniaturization of body size: Organismal consequences and evolutionary significance. *Annu Rev Ecol Syst* 24:501–519.
6. Brown R (1822) An account of a new genus of plants, named *Rafflesia*. *Trans Linn Soc (Lond)* 13:201–236.
7. Brown R (1845) Description of the female flower and fruit of *Rafflesia arnoldi* with remarks on its affinities; and an illustration of the structure of *Hydnora africana*. *Trans Linn Soc (Lond)* 19:221–239.
8. Barkman TJ, Lim SH, Salleh KM, Nais J (2004) Mitochondrial DNA sequences reveal the photosynthetic relatives of *Rafflesia*, the world's largest flower. *Proc Natl Acad Sci USA* 101(3):787–792.
9. Davis CC, Latvis M, Nickrent DL, Wurdack KJ, Baum DA (2007) Floral gigantism in Rafflesiaceae. *Science* 315(5820):1812.
10. Wurdack KJ, Davis CC (2009) Malpighiales phylogenetics: Gaining ground on one of the most recalcitrant clades in the angiosperm tree of life. *Am J Bot* 96(8):1551–1570.
11. Proctor M, Yeo P, Lack A (2003) *The Natural History of Pollination* (Timber Press, Portland, OR).
12. Davis CC, Endress PK, Baum DA (2008) The evolution of floral gigantism. *Curr Opin Plant Biol* 11(1):49–57.
13. Beaman R, Decker P, Beaman J (1988) Pollination of *Rafflesia* (Rafflesiaceae). *Am J Bot* 75(8):1148–1162.
14. Bänziger H, Hansen B (1997) Unmasking the real identity of *Sapria poilanei* Gagnepain emend., and description of *Sapria ram* sp. n. (Rafflesiaceae). *Nat Hist Bull Siam Soc* 45:149–170.
15. Bendiksby M, et al. (2010) Elucidating the evolutionary history of the Southeast Asian, holoparasitic, giant-flowered Rafflesiaceae: Pliocene vicariance, morphological convergence and character displacement. *Mol Phylogenet Evol* 57(2):620–633.
16. Bänziger H, Hansen B (2000) A new taxonomic revision of the deceptive flower, *Rhizanthes* Dumortier (Rafflesiaceae). *Nat Hist Bull Siam Soc* 48(1):117–144.
17. Litt A, Kramer EM (2010) The ABC model and the diversification of floral organ identity. *Semin Cell Dev Biol* 21(1):129–137.
18. Smaczniak C, Immink RG, Angenent GC, Kaufmann K (2012) Developmental and evolutionary diversity of plant MADS-domain factors: Insights from recent studies. *Development* 139(17):3081–3098.
19. Irish VF, Litt A (2005) Flower development and evolution: Gene duplication, diversification and redeployment. *Curr Opin Genet Dev* 15(4):454–460.
20. Kramer EM, Irish VF (2000) Evolution of the petal and stamen developmental programs: Evidence from comparative studies of the lower eudicots and basal angiosperms. *Int J Plant Sci* 161(6 Suppl.):S29–S40.
21. Jaramillo MA, Kramer EM (2007) The role of developmental genetics in understanding homology and morphological evolution in plants. *Int J Plant Sci* 168(1): 61–72.
22. Brockington SF, et al. (2012) 'Living stones' reveal alternative petal identity programs within the core eudicots. *Plant J* 69(2):193–203.
23. Waters MT, et al. (2013) The corona of the daffodil *Narcissus bulbocodium* shares stamen-like identity and is distinct from the orthodox floral whorls. *Plant J* 74(4): 615–625.
24. Hemingway CA, Christensen AR, Malcomber ST (2011) B- and C-class gene expression during corona development of the blue passionflower (*Passiflora caerulea*, Passifloraceae). *Am J Bot* 98(6):923–934.
25. Kramer EM, Hall JC (2005) Evolutionary dynamics of genes controlling floral development. *Curr Opin Plant Biol* 8(1):13–18.
26. Jiao Y, et al. (2012) A genome triplication associated with early diversification of the core eudicots. *Genome Biol* 13(1):R3.
27. Endress PK, Matthews ML (2006) Elaborate petals and staminodes in eudicots: Diversity, function, and evolution. *Org Divers Evol* 6(4):257–293.
28. Kaufmann K, Melzer R, Theissen G (2005) MIKC-type MADS-domain proteins: Structural modularity, protein interactions and network evolution in land plants. *Gene* 347(2):183–198.
29. Jaramillo MA, Kramer EM (2004) *APETALA3* and *PISTILLATA* homologs exhibit novel expression patterns in the unique perianth of *Aristolochia* (Aristolochiaceae). *Evol Dev* 6(6):449–458.
30. Ambrose BA, et al. (2000) Molecular and genetic analyses of the *silky1* gene reveal conservation in floral organ specification between eudicots and monocots. *Mol Cell* 5(3):569–579.
31. Álvarez-Buylla ER, et al. (2010) B-function expression in the flower center underlies the homeotic phenotype of *Lacandonia schismatica* (Triuridaceae). *Plant Cell* 22(11): 3543–3559.
32. Barcelona J, Pelser P, Balete D, Co L (2009) Taxonomy, ecology, and conservation status of Philippine *Rafflesia* (Rafflesiaceae). *Blumea* 54(1-3):77–93.
33. Griffith W (1845) On the root-parasites referred by authors to Rhizantheae; And on various plants related to them. *Trans Linn Soc (Lond)* 19:303–348.
34. Bolin J, Maass E, Musselman L (2009) Pollination biology of *Hydnora africana* Thunb. (Hydnoraceae) in Namibia: Brood site mimicry with insect imprisonment. *Int J Plant Sci* 170(2):157–163.
35. True JR, Haag ES (2001) Developmental system drift and flexibility in evolutionary trajectories. *Evol Dev* 3(2):109–119.
36. Liu PZ, Kaufman TC (2005) Short and long germ segmentation: Unanswered questions in the evolution of a developmental mode. *Evol Dev* 7(6):629–646.
37. Bentley D, Keshishian H, Shankland M, Toroian-Raymond A (1979) Quantitative staging of embryonic development of the grasshopper, *Schistocerca nitens*. *J Embryol Exp Morphol* 54:47–74.
38. Sommer RJ (2012) *Evolutionary Systems Biology*, ed Soyer O (Springer, Heidelberg), pp 79–92.
39. Barkman TJ, et al. (2008) Accelerated rates of floral evolution at the upper size limit for flowers. *Curr Biol* 18(19):1508–1513.
40. Litt A, Irish VF (2003) Duplication and divergence in the *APETALA1/FRUITFULL* gene lineage: Implications for the evolution of floral development programs. *Genetics* 165(2):821–833.
41. Stellari GM, Jaramillo MA, Kramer EM (2004) Evolution of the *APETALA3* and *PISTILLATA* lineages of MADS-box-containing genes in the basal angiosperms. *Mol Biol Evol* 21(3): 506–519.

Supporting Information

Nikolov et al. 10.1073/pnas.1310356110

SI Materials and Methods

Phylogenetic Inference of Gene Family Evolution. Predicted amino acid sequences were aligned with broadly sampled sequences from different MIKC-MADS box lineages and from different plant species (Table S1). The best-scoring maximum-likelihood tree was obtained using RAxML (1) with an LG amino acid substitution model (2), and 1,000 bootstrap replicates were estimated using the rapid bootstrap algorithm (3). The bootstrap percentages were summarized from all 1,000 bootstrap trees, and the bipartition tree was obtained by mapping these bootstrap percentages to the best-scoring maximum-likelihood tree.

Microscopy and Image Analysis. For scanning electron microscopy, fixed young floral buds and selected organs were dissected and postfixed in 2% OsO_4 for 2 h, then critically point dried using Samdri-PVT-3D (Tousimis Research). The dried specimens were mounted and sputter-coated with Pd/Pt at 20 mA or Pt/Au at 40 mA for 180 s. The stubs were examined with EVO-SEM at 10.00 keV and image brightness and contrast were uniformly adjusted in Photoshop.

Histology. Specimens were embedded in Kulzer's Technovit (2-hydroethyl methacrylate) for serial microtome sections. A stepwise infiltration was performed with 50:50, 25:75, and 0:100 ratios of 100% ethanol (vol/vol) to Technovit solution. Embedded material was sectioned using a Microm HM 355 Rotary microtome with a conventional knife D. The 7-μm-thick sections were stained with Ruthenium red and Toluidine blue and mounted in Histomount (Invitrogen). Permanent slides of the microtome sections are deposited at the Harvard University Herbaria (A).

1. Stamatakis A (2006) RAxML-VI-HPC: Maximum likelihood-based phylogenetic analyses with thousands of taxa and mixed models. *Bioinformatics* 22(21):2688–2690.
2. Le SQ, Gascuel O (2008) An improved general amino acid replacement matrix. *Mol Biol Evol* 25(7):1307–1320.
3. Stamatakis A, Hoover P, Rougemont J (2008) A rapid bootstrap algorithm for the RAxML Web servers. *Syst Biol* 57(5):758–771.

Fig. S1. Illustrations of *Rafflesia cantleyi* (*A* and *B*), *Sapria himalayana* (*C–F*), and *Rhizanthes lowii* (*G–K*). (*A*) Longitudinal section of an open male *Rafflesia* flower, showing the floral chamber enclosing the central disk (cd); ramenta (ra) line the inner surface of the chamber. (*B*) Central disk (cd) of *Rafflesia* with ring (blue); perianth tube (yellow) and bracts (red) have been removed. (*C*) Longitudinal section of an open male *Sapria* flower, showing the floral chamber enclosing the central disk (cd); ramenta (ra) are found on top of the diaphragm. (*D*) Longitudinal section of an advanced female bud of *Sapria*, showing the position of the ovary (ov) and the longitudinal grooves and ridges. (*E*) Longitudinal section of an advanced male bud of *Sapria*, showing the partitioning of the floral chamber into two compartments by the diaphragm (dia). (*F*) Detail of the ramenta on the upper surface of the diaphragm in *Sapria*. (*G*) Longitudinal section of an open male *Rhizanthes* flower, showing the exposed central disk. (*H*) Detail of the pads on the perianth lobes in *Rhizanthes*. (*I*) Longitudinal section of an advanced female bud of *Rhizanthes*, showing the position of the ovary; tails are removed. (*J*) Longitudinal section of an advanced male bud of *Rhizanthes* with tails (ta) shown (ovarial locules without functional ovules present). (*K*) Detail of the pads on the perianth lobes of an open *Rhizanthes* flower relative to the perianth tube, which is the region below the band of long hairs.

Fig. S1 (PDF)

Fig. S2. Gene trees of MADS-box sequences from Rafflesiaceae and outgroup families. Sequences generated for this study are in red. Maximum likelihood support above 50% is indicated at the nodes. (*A*) MADS box gene tree based on the MADS intervening keratin-like (MIK) domains, with gene lineages colored as follows: A- (yellow), B- (blue), C-/D- (red), and E-class (green). (*B*) *GLOBOSA*-like genes. (*C*) *DEFICIENS*-like genes. *Inset* in the upper left corner depicts the consensus on the duplication history of the locus in angiosperms [after Jaramillo and Kramer (1)]. (*D*) *AGAMOUS*-like genes. *Inset* in the upper left corner depicts the consensus on the duplication history of the locus in angiosperms [after Jaramillo and Kramer (1)]. (*E*) *SQUAMOSA*-like genes. *Inset* in the upper left corner depicts the consensus on the duplication history of the locus in angiosperms [after Litt and Irish (2)]. (*F*) *SEPALLATA*-like genes.

Fig. S2 (PDF)

1. Jaramillo MA, Kramer EM (2007) The role of developmental genetics in understanding homology and morphological evolution in plants. *Int J Plant Sci* 168(1):61–72.
2. Litt A, Irish VF (2003) Duplication and divergence in the APETALA1/FRUITFULL gene lineage: Implications for the evolution of floral development programs. *Genetics* 165(2):821–833.

Fig. S3. PaleoAP3 and euAP3 C-terminal motifs of *DEF*-like genes from Rafflesiaceae and outgroups. Note the extensive stretch of amino acids preceding the paleoAP3 motif in the *TM6* homologs of Rafflesiaceae (gray shading).

Fig. S3 (PDF)

Fig. S4. Sampling scheme for *Rafflesia* (*A*), *Sapria* (*B*) and *Rhizanthes* (*C*). Labels correspond to those in Fig. 2: Br, bracts; Bs, base of the flower; Dia, diaphragm; Dsk, disk; Lb, perianth lobes; ; Ov, ovary; St, stamens; Tb, perianth tube. Taxon-specific regions for *Rafflesia*: Flr, floor of the floral chamber. Taxon-specific regions for *Sapria*: In, inner perianth lobes; Out, outer perianth lobes. Taxon-specific regions for *Rhizanthes*: Tl, tails, PrD, E and F, levels indicated in Fig. S6*C*. Note that because of their alternate positions in *Sapria*, an outer perianth lobe is depicted on the left side and an inner perianth lobe is depicted on the right side of the longitudinal section of the flower.

Fig. S4 (PDF)

Fig. S5. MADS-box gene expression in Rafflesiaceae and *Clutia* (Peraceae). Actin is used as a concentration control. Column labeling corresponds to the floral regions in Fig. S4. (*A*) *Rafflesia* MADS-box genes. *RfSTK* is expressed in two splice variants, with or without exon 6, which generates two bands in RT-PCR. (*B*) *Sapria* MADS-box genes. (*C*) *Rhizanthes TM6*. (*D*) Expression of MADS-box genes in *Clutia* flowers: Car, carpels; Pe, petals; Se, sepals. Primers are not designed to discriminate between the duplicate copies/alleles of *CluPI* (yellow), *CluTM6* and *CluAG* (blue). Gray shading indicates the uncertainty in the gene expression profile of *Clutia* nectaries.

Fig. S5 (PDF)

Fig. S6. Light microscopy images of sections of buds of *Rafflesia* (*A*) and *Rhizanthes* (*B*–*G*). (*A*) Longitudinal section of *Rafflesia* bud, showing the appearance of stamens (asterisk) and the ring structure outside of the stamens (arrowheads). (*B*) Longitudinal section of a *Rhizanthes* bud, showing the growth of the ring (arrowhead); fusion (not certain to what extent congenital or postgenital) between the ring and the perianth lobe is depicted by arrows. A stamen is marked with an asterisk. (*C*) Longitudinal section of an advanced *Rhizanthes* bud; dotted lines along the right side of the section correspond to the transverse sections shown in *D*–*G*. Adnation of the ring derivative to the perianth lobe, at levels D–F, is depicted by arrows; level G is at the perianth tube. A stamen is marked with an asterisk. (*D*) Transverse section at the level where the perianth lobes are completely free and arc inwards toward the central column to form the tails. Arrows indicate the adnation of the perianth lobes with the distal end of the ring derivative. (*E*) Transverse section at the level of the pads. Fusion between the pads and the perianth is discernible (arrows); a complete dissection of this compound structure is indicated with a dashed line. (*F*) Transverse section at the level where the pads fuse laterally to form an uninterrupted band (black dots) on the inner side of the perianth lobes, which remain free (dashed line). Fusion between the pads and the perianth lobes is still noticeable (arrows). (*G*) Transverse section through the perianth tube, which is more homogeneous and no dissection or fusion is observed. (Scale bars, 500 μm.)

Fig. S6 (PDF)

Fig. S7. Evolutionary models for the possible origin of floral chambers in Rafflesiaceae. (*A*) Independent origin of floral chambers in *Sapria* and *Rafflesia*, in which the common ancestor lacked chamber closure. (*B*) Origin of a *Rafflesia*-like floral chamber from a *Sapria*-like floral chambered ancestor via developmental system drift with the loss of the floral chamber in *Rhizanthes*. (*C*) A model where the common ancestor of Rafflesiaceae possessed a floral chamber, which was lost in the common ancestor of *Rafflesia* + *Rhizanthes*. Subsequently, a floral chamber with different organization re-evolved in *Rafflesia*.

Fig. S7 (PDF)

Other Supporting Information Files

Table S1 (DOCX)
Table S2 (DOCX)

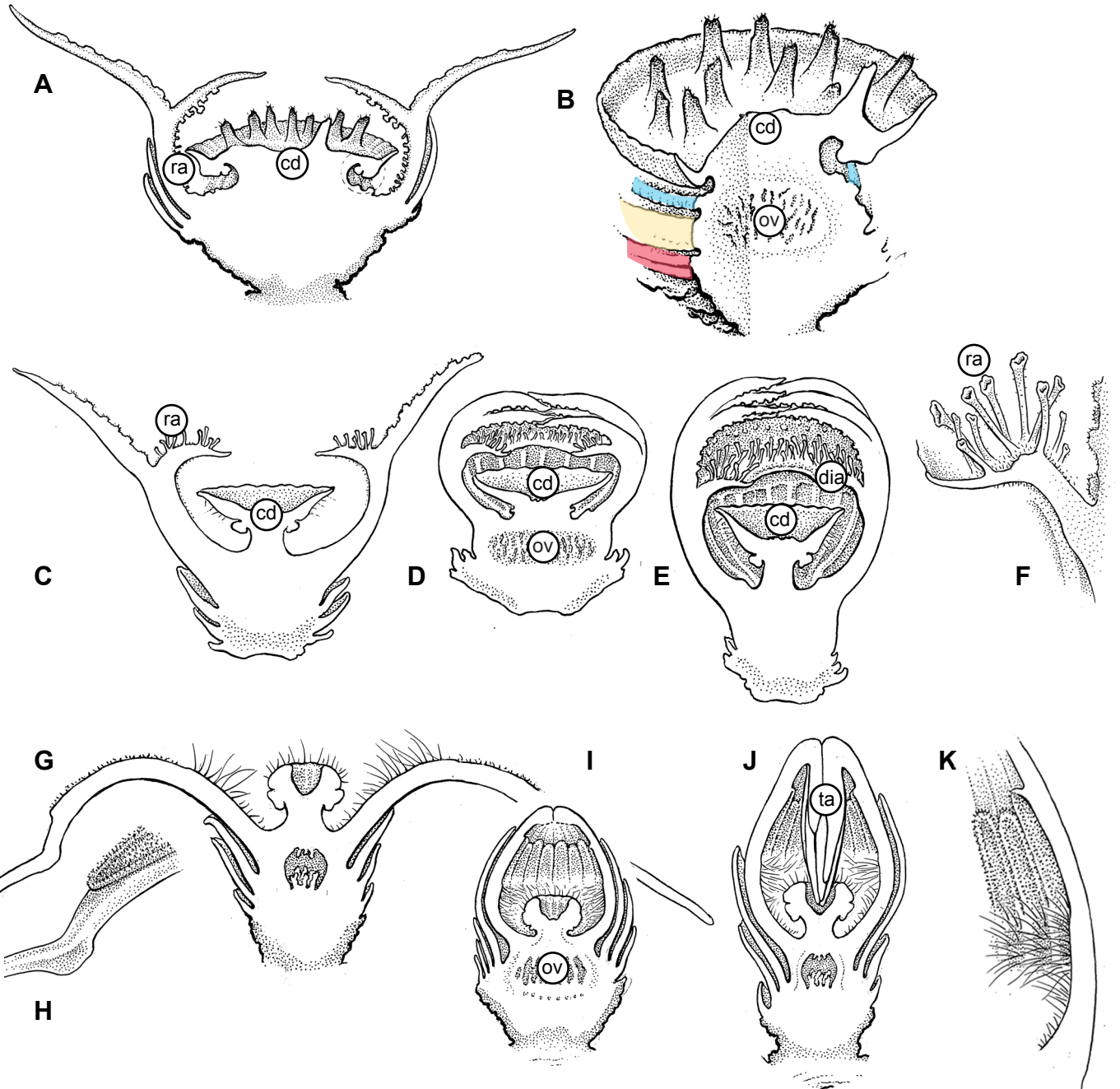
A
ra
cd
B
cd
ov
C
ra
cd
D
cd
ov
E
dia
cd
F
ra
G
H
I
ov
J
ta
K

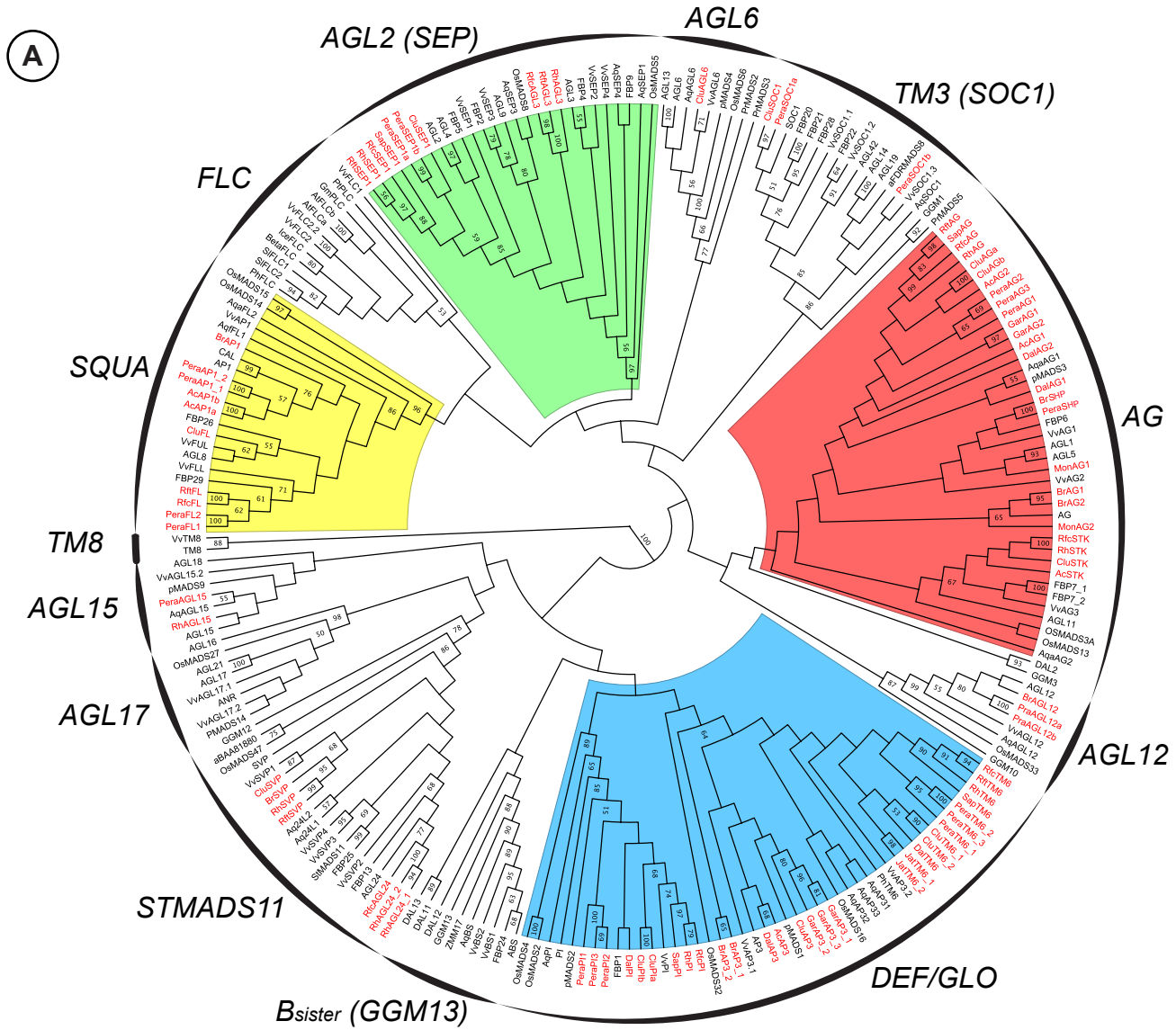
A
AGL2 (SEP)
AGL6
TM3 (SOC1)
FLC
SQUA
AG
TM8
AGL15
AGL17
AGL12
STMADS11
DEF/GLO
Bsister (GGM13)

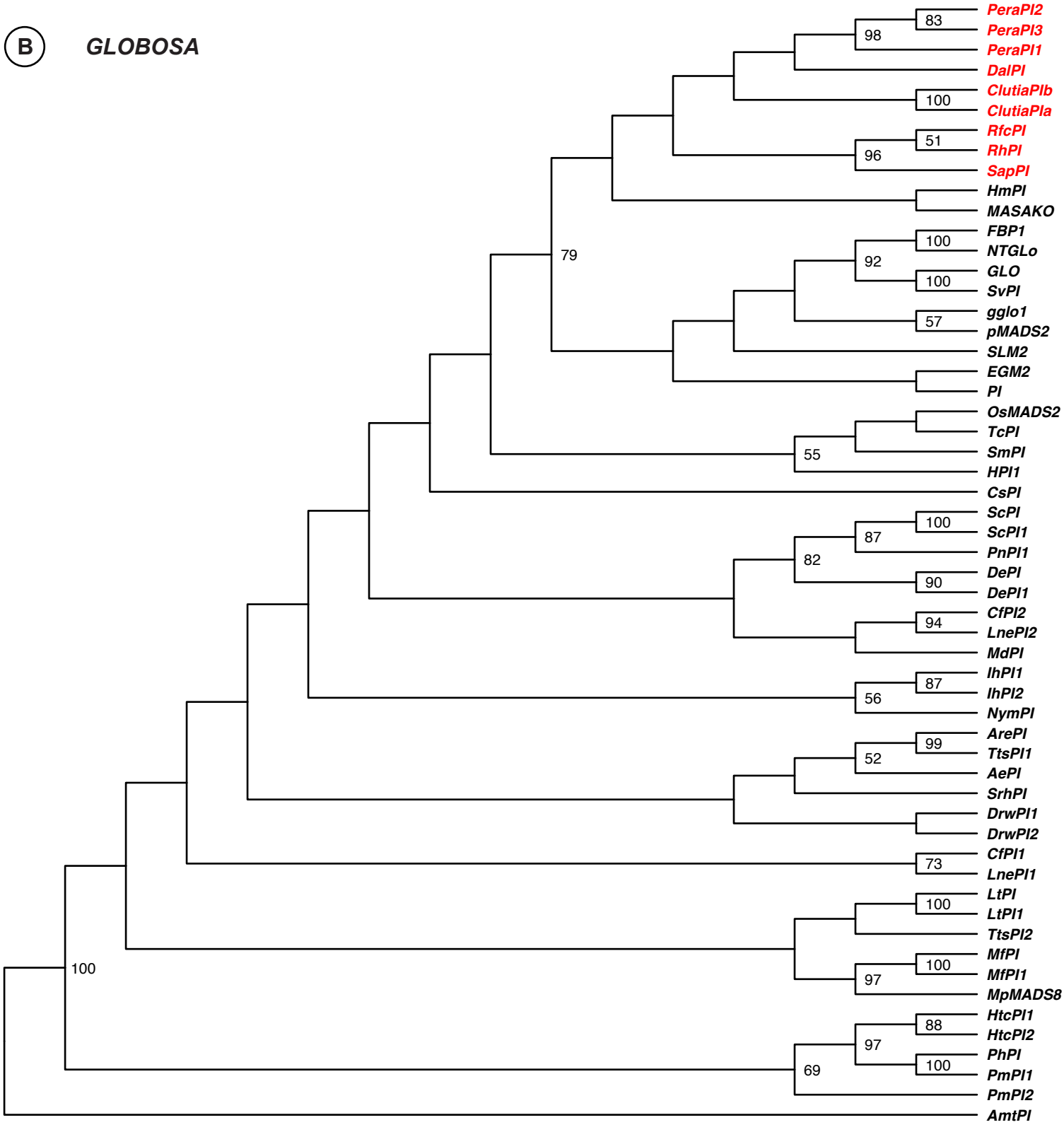
B
GLOBOSA
PeraPI2
PeraPI3
PeraPI1
DalPI
ClutiaPIb
ClutiaPIa
RfcPI
RhPI
SapPI
HmPI
MASAKO
FBP1
NTGLo
GLO
SvPI
gglo1
pMADS2
SLM2
EGM2
PI
OsMADS2
TcPI
SmPI
HPI1
CsPI
ScPI
ScPI1
PnPI1
DePI
DePI1
CfPI2
LnePI2
MdPI
IhPI1
IhPI2
NymPI
ArePI
TtsPI1
AePI
SrhPI
DrwPI1
DrwPI2
CfPI1
LnePI1
LtPI
LtPI1
TtsPI2
MfPI
MfPI1
MpMADS8
HtcPI1
HtcPI2
PhPI
PmPI1
PmPI2
AmtPI
83
98
100
51
96
79
100
92
100
57
55
100
87
82
90
94
87
56
99
52
73
100
97
100
88
97
100
69
100

C

DEFICIENS

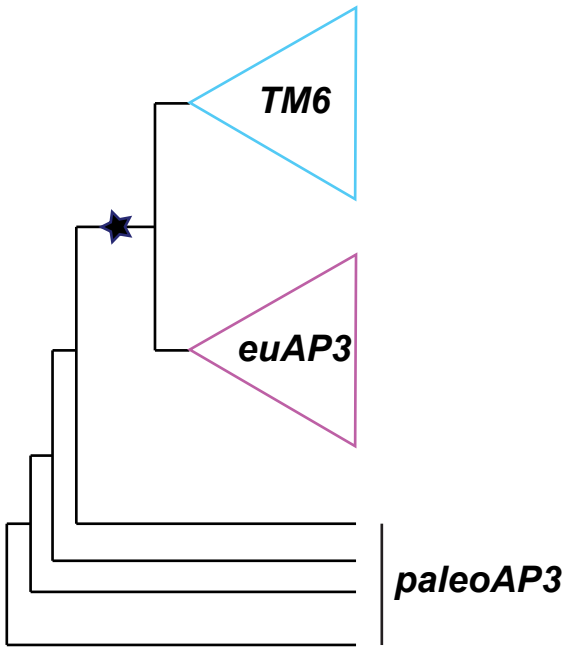

PhTM6
TM6
DiiTM6
DalAP3_1
MtAP3
LodTM6
PeraTM6_2
PeraTM6_3
PeraTM6_1
PhaTM6.1
PhaTM6.2
GumTM6.2
GumTM6.3
GumTM6.1
SxcTM6
CosTM6.1
CosTM6.2
JatTM6_1
JatTM6_2
CluTM6_1
CluTM6_2
RfcTM6
RftTM6
RhTM6
SapTM6
PTD
MadMdTM6
MdMADS13
HaM91
VvTM6
BuxAP3.1
HAM2
HAM63
DcMADS3
SLM3
AcAP3
DalAP3_2
AP3
CsMADS1
GarAP3_1
GarAP3_2
GarAP3_3
ClutiaAP3
DEFA
SvAP3
GP
TAP3
IhDEF1
IhDEF2
DiiAP3
VvAP3
BpMADS8
CosAP3
SxcAP3
BuxAP3.2
BuxAP3.3
PtAP3.1
PtAP3.2
BrAP3_1
BrAP3_2
TraAP3
PaAP3
PloAP3.2
PloAP3.1
AqaAP3.2
EcDEF2
PnAP3.1
AqaAP3.1
EcDEF1
PnAP3.2
DeAP3
MdAP3.1
MdAP3.3
MdAP3.2
AqaAP3.3
NnAP3
DrwAP3.1
DrwAP3.2
DrwAP3.3
DrwAP3.4
CfAP3.2
Peam.AP3
CfAP3.1
MpMADS7
AODEF
DcOAP3A
DcOAP3B
LMADS1
OsMADS16
CsAP3
IlflAP31
AmAP3
IlflAP32
IlflAP33
NuadAP31
NuadAP32
HtcAP3
NjPI.1
NjPI.2
AmPI

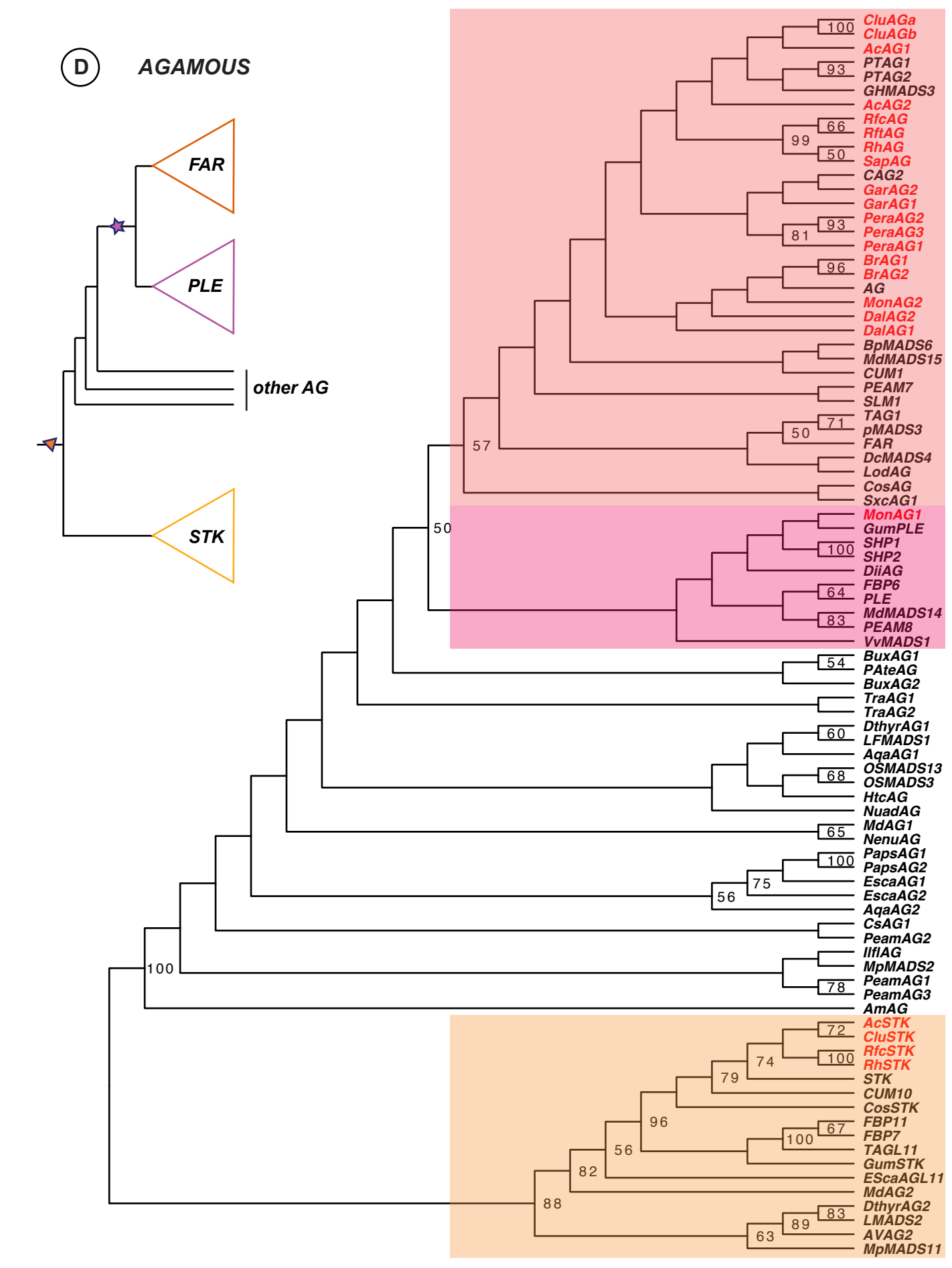
D
AGAMOUS
FAR
PLE
other AG
STK
CluAGa
CluAGb
AcAG1
PTAG1
PTAG2
GHMADS3
AcAG2
RfcAG
RftAG
RhAG
SapAG
CAG2
GarAG2
GarAG1
PeraAG2
PeraAG3
PeraAG1
BrAG1
BrAG2
AG
MonAG2
DalAG2
DalAG1
BpMADS6
MdMADS15
CUM1
PEAM7
SLM1
TAG1
pMADS3
FAR
DcMADS4
LodAG
CosAG
SxcAG1
MonAG1
GumPLE
SHP1
SHP2
DiiAG
FBP6
PLE
MdMADS14
PEAM8
VvMADS1
BuxAG1
PAteAG
BuxAG2
TraAG1
TraAG2
DthyrAG1
LFMADS1
AqaAG1
OSMADS13
OSMADS3
HtcAG
NuadAG
MdAG1
NenuAG
PapsAG1
PapsAG2
EscaAG1
EscaAG2
AqaAG2
CsAG1
PeamAG2
IlflAG
MpMADS2
PeamAG1
PeamAG3
AmAG
AcSTK
CluSTK
RfcSTK
RhSTK
STK
CUM10
CosSTK
FBP11
FBP7
TAGL11
GumSTK
EScaAGL11
MdAG2
DthyrAG2
LMADS2
AVAG2
MpMADS11
100
93
66
99
50
93
81
96
71
50
57
50
54
60
68
65
100
75
56
100
72
100
74
79
96
67
100
56
82
88
83
89
63
78

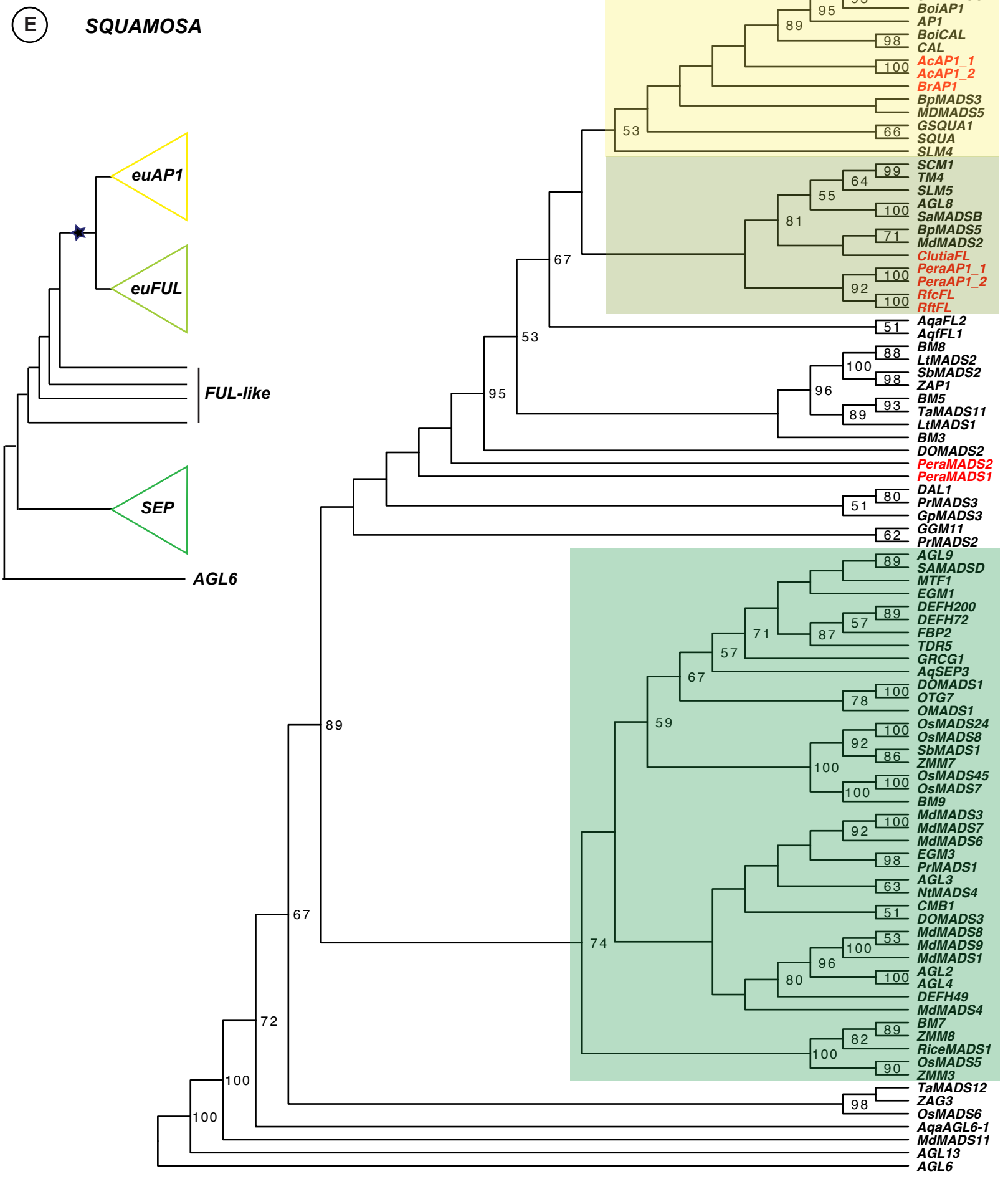
E
SQUAMOSA
euAP1
euFUL
FUL-like
SEP
AGL6
BoAP1
SAMADSC2
BoiAP1
AP1
BoiCAL
CAL
AcAP1_1
AcAP1_2
BrAP1
BpMADS3
MDMADS5
GSQUA1
SQUA
SLM4
SCM1
TM4
SLM5
AGL8
SaMADSB
BpMADS5
MdMADS2
ClutiaFL
PeraAP1_1
PeraAP1_2
RfcFL
RftFL
AqaFL2
AqfFL1
BM8
LtMADS2
SbMADS2
ZAP1
BM5
TaMADS11
LtMADS1
BM3
DOMADS2
PeraMADS2
PeraMADS1
DAL1
PrMADS3
GpMADS3
GGM11
PrMADS2
AGL9
SAMADSD
MTF1
EGM1
DEFH200
DEFH72
FBP2
TDR5
GRCG1
AqSEP3
DOMADS1
OTG7
OMADS1
OsMADS24
OsMADS8
SbMADS1
ZMM7
OsMADS45
OsMADS7
BM9
MdMADS3
MdMADS7
MdMADS6
EGM3
PrMADS1
AGL3
NtMADS4
CMB1
DOMADS3
MdMADS8
MdMADS9
MdMADS1
AGL2
AGL4
DEFH49
MdMADS4
BM7
ZMM8
RiceMADS1
OsMADS5
ZMM3
TaMADS12
ZAG3
OsMADS6
AqaAGL6-1
MdMADS11
AGL13
AGL6

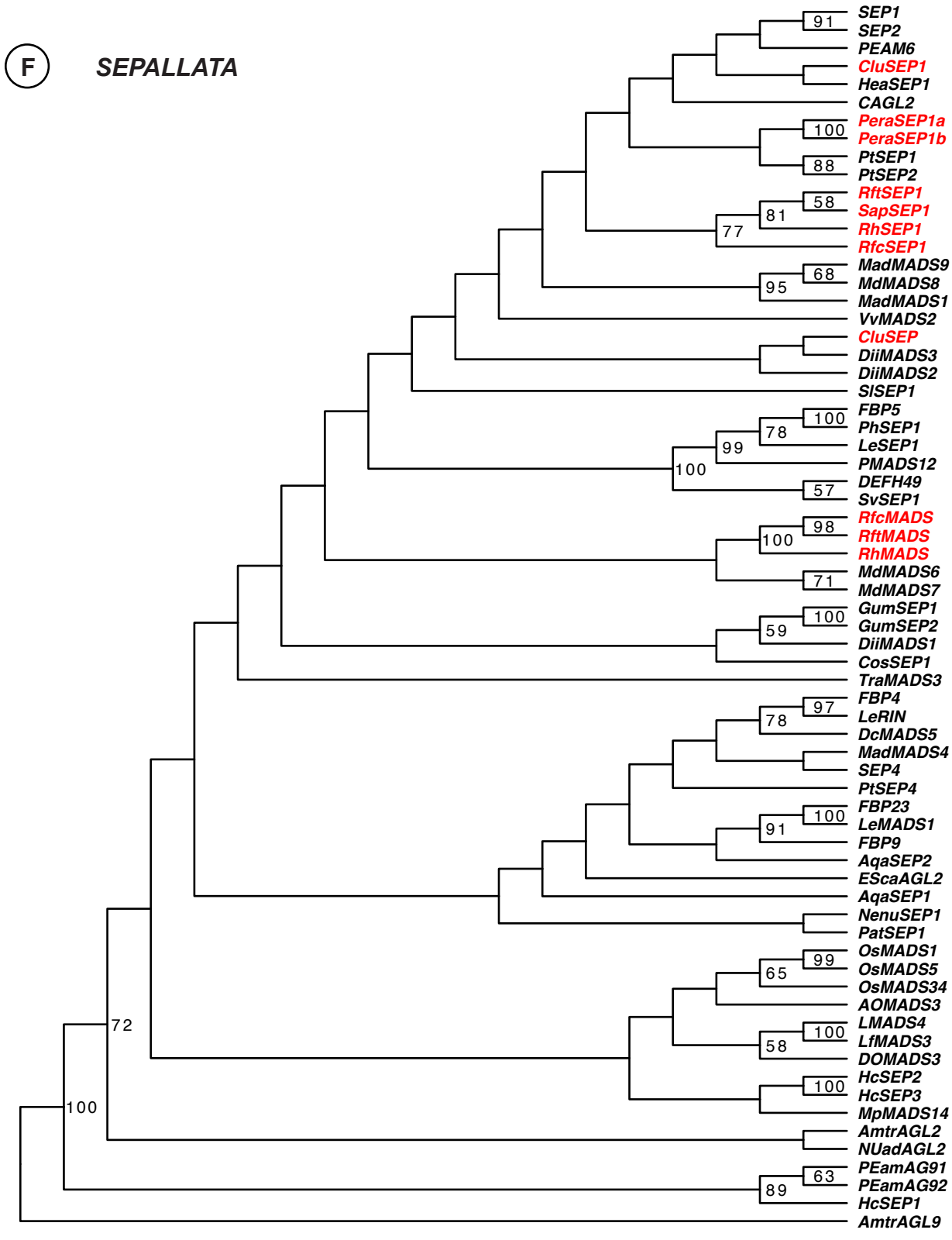
F
SEPALLATA
SEP1
SEP2
PEAM6
CluSEP1
HeaSEP1
CAGL2
PeraSEP1a
PeraSEP1b
PtSEP1
PtSEP2
RftSEP1
SapSEP1
RhSEP1
RfcSEP1
MadMADS9
MdMADS8
MadMADS1
VvMADS2
CluSEP
DiiMADS3
DiiMADS2
SlSEP1
FBP5
PhSEP1
LeSEP1
PMADS12
DEFH49
SvSEP1
RfcMADS
RftMADS
RhMADS
MdMADS6
MdMADS7
GumSEP1
GumSEP2
DiiMADS1
CosSEP1
TraMADS3
FBP4
LeRIN
DcMADS5
MadMADS4
SEP4
PtSEP4
FBP23
LeMADS1
FBP9
AqaSEP2
EScaAGL2
AqaSEP1
NenuSEP1
PatSEP1
OsMADS1
OsMADS5
OsMADS34
AOMADS3
LMADS4
LfMADS3
DOMADS3
HcSEP2
HcSEP3
MpMADS14
AmtrAGL2
NUadAGL2
PEamAG91
PEamAG92
HcSEP1
AmtrAGL9
91
100
88
58
81
77
68
95
100
78
99
100
57
98
100
71
100
59
97
78
100
91
99
65
100
58
100
72
100
63
89

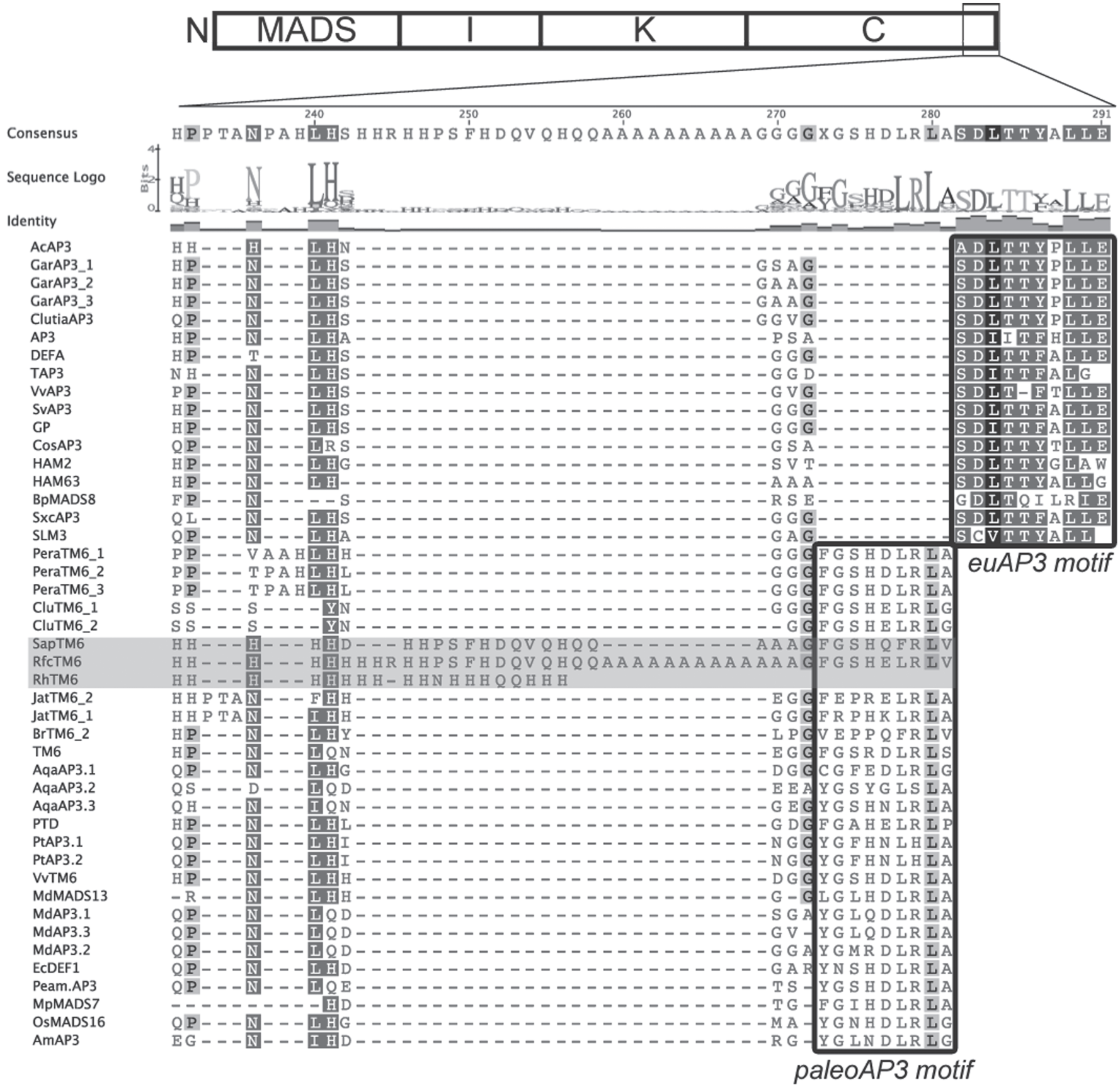
N
MADS
I
K
C
240
250
260
270
280
291
Consensus
Sequence Logo
Bits
Identity
AcAP3
GarAP3_1
GarAP3_2
GarAP3_3
ClutiaAP3
AP3
DEFA
TAP3
VvAP3
SvAP3
GP
CosAP3
HAM2
HAM63
BpMADS8
SxcAP3
SLM3
PeraTM6_1
PeraTM6_2
PeraTM6_3
CluTM6_1
CluTM6_2
SapTM6
RfcTM6
RhTM6
JatTM6_2
JatTM6_1
BrTM6_2
TM6
AqaAP3.1
AqaAP3.2
AqaAP3.3
PTD
PtAP3.1
PtAP3.2
VvTM6
MdMADS13
MdAP3.1
MdAP3.3
MdAP3.2
EcDEF1
Peam.AP3
MpMADS7
OsMADS16
AmAP3
euAP3 motif
paleoAP3 motif

A *Rafflesia*

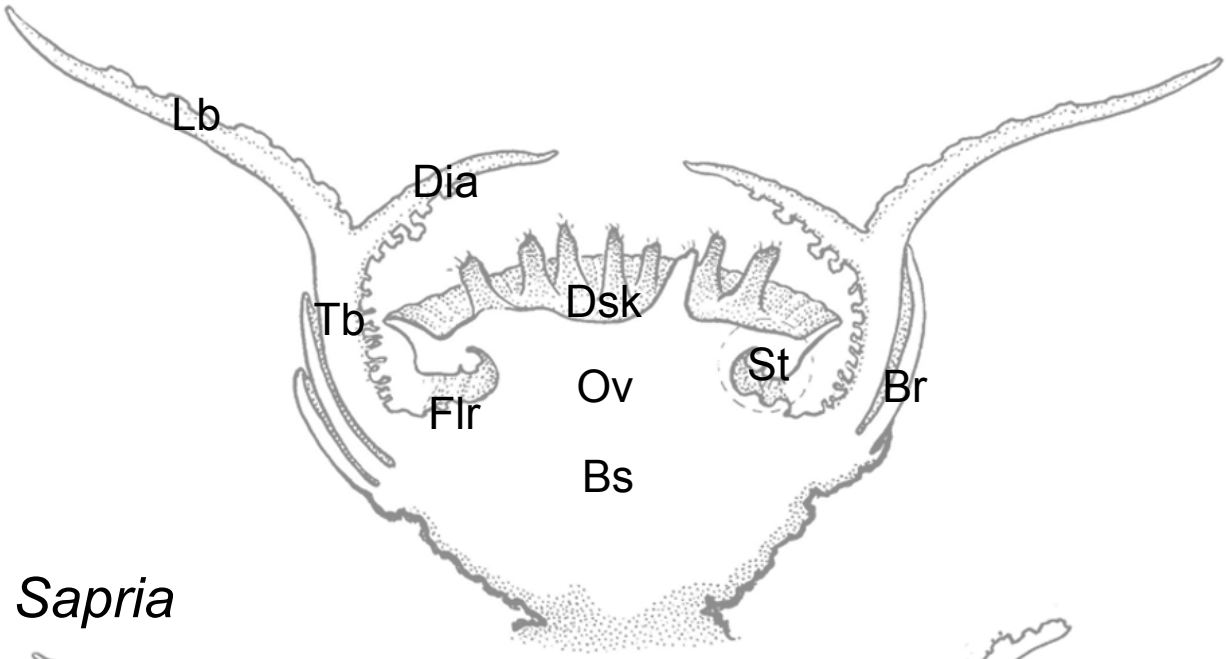

B *Sapria*

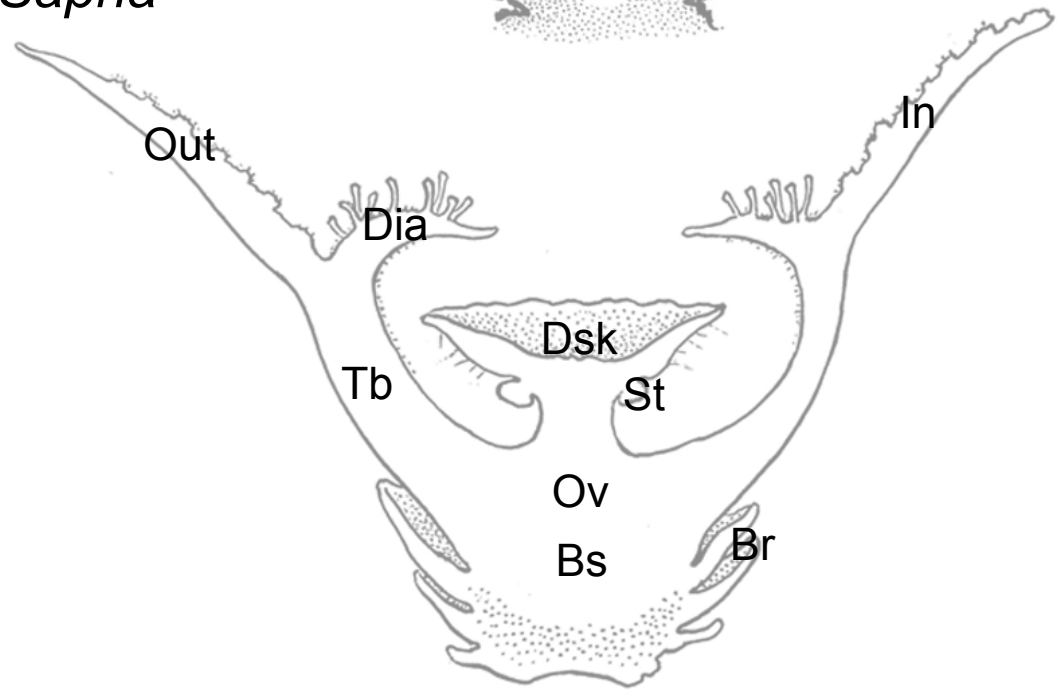

C *Rhizanthes*

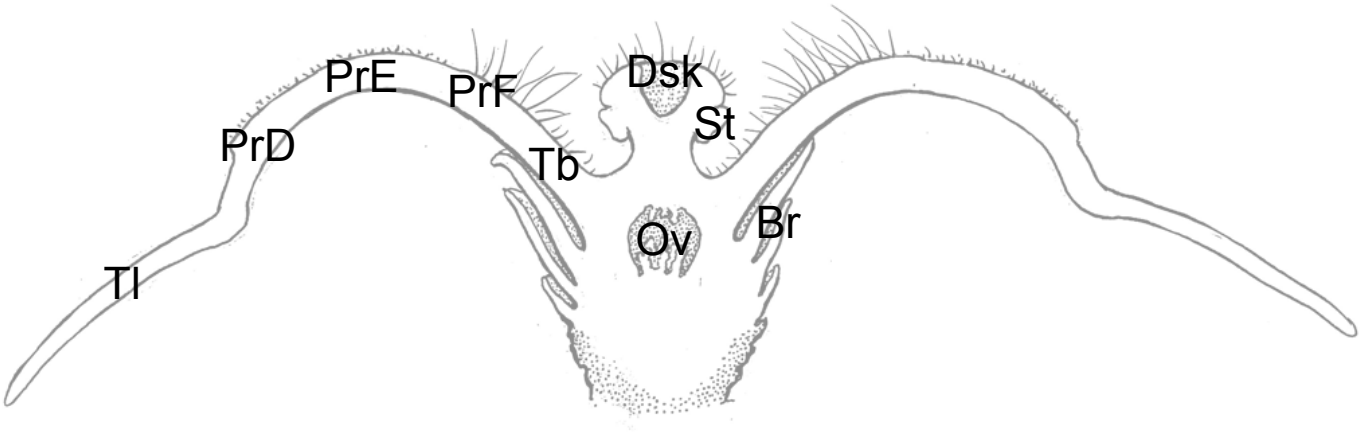

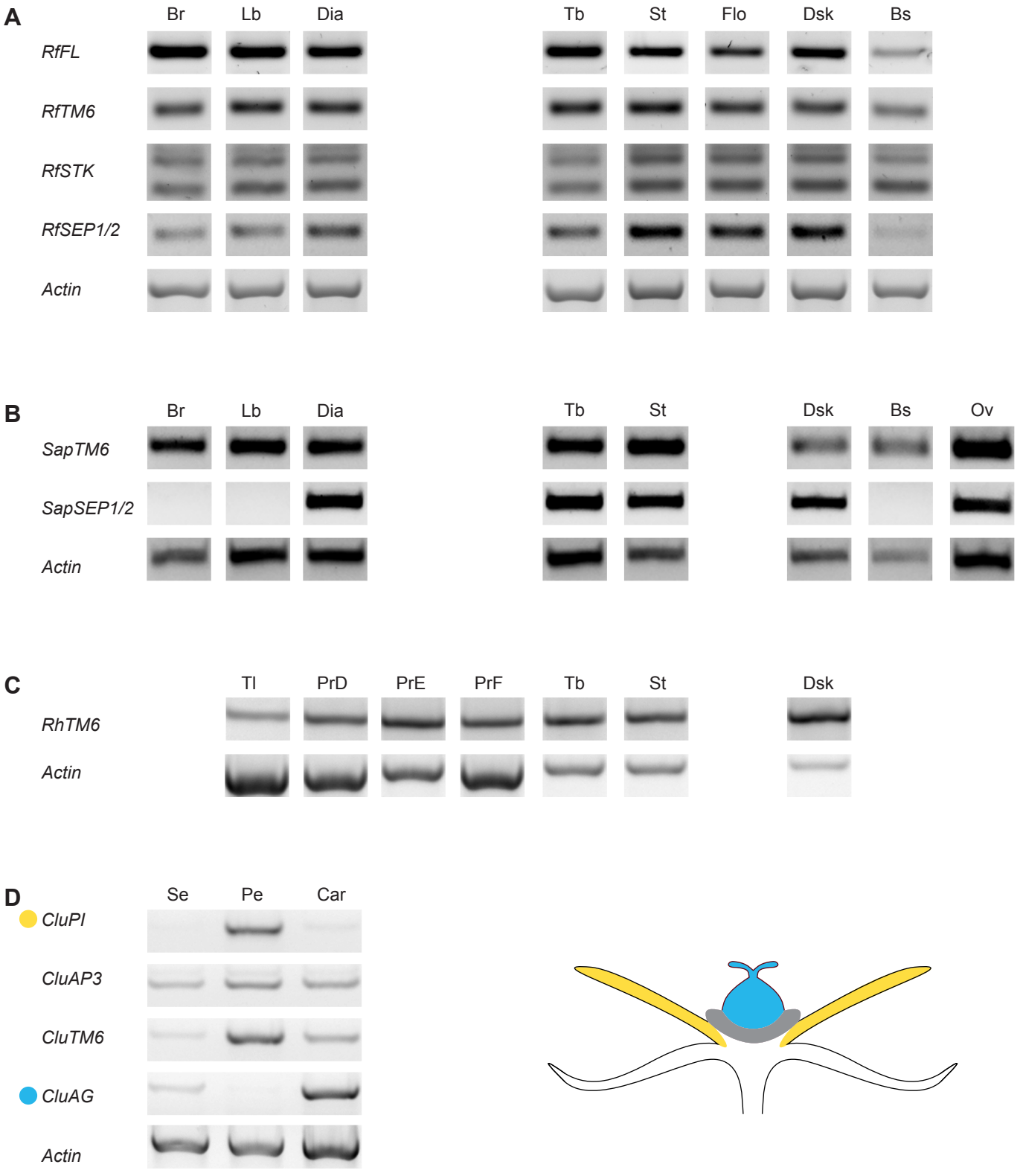
A
Br
Lb
Dia
Tb
St
Flo
Dsk
Bs
RfFL
RfTM6
RfSTK
RfSEP1/2
Actin
B
Br
Lb
Dia
Tb
St
Dsk
Bs
Ov
SapTM6
SapSEP1/2
Actin
C
Tl
PrD
PrE
PrF
Tb
St
Dsk
RhTM6
Actin
D
Se
Pe
Car
CluPI
CluAP3
CluTM6
CluAG
Actin

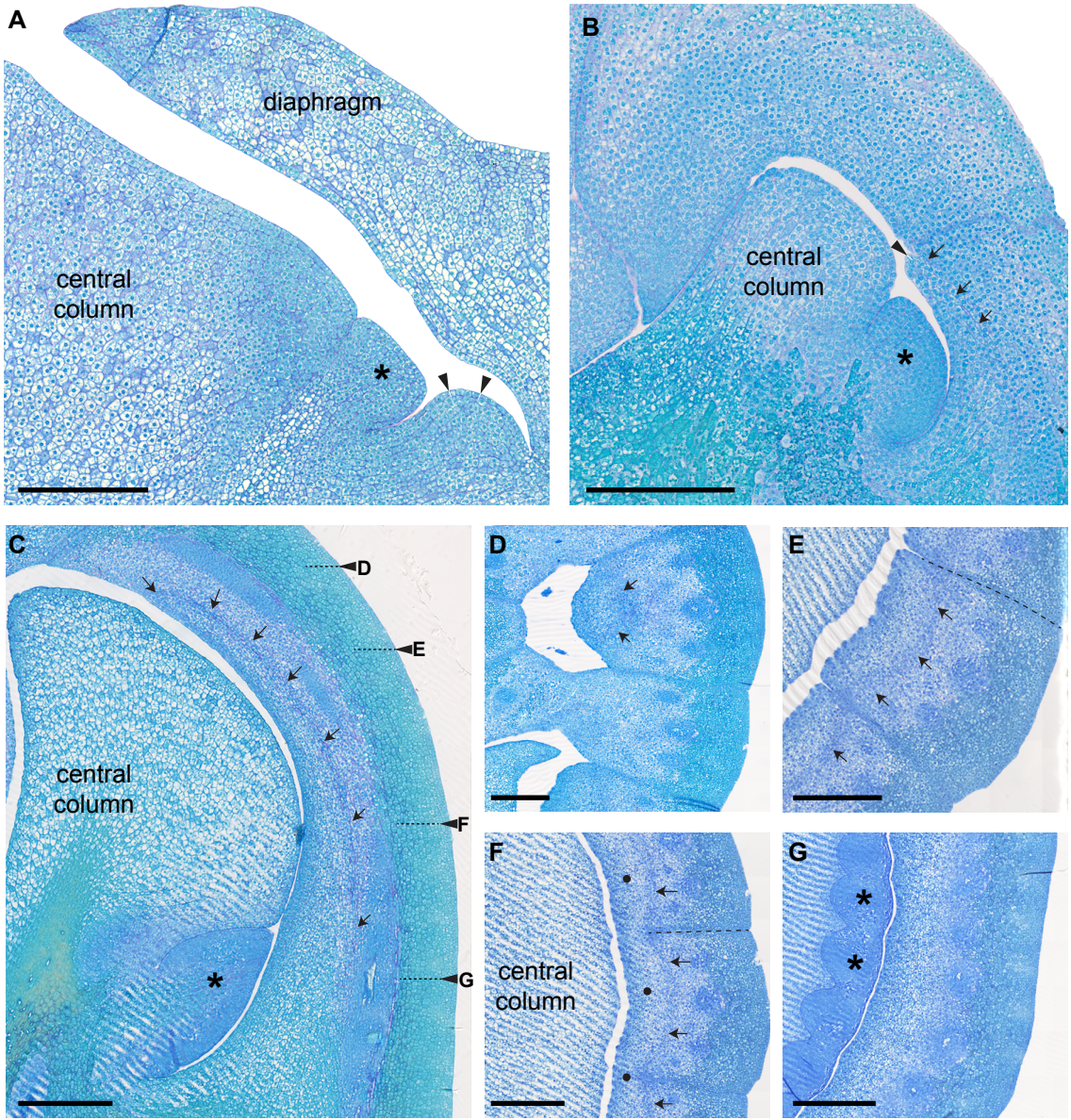
A
diaphragm
central
column
*
B
central
column
*
C
D
E
F
G
central
column
*
D
E
F
central
column
G
*
*

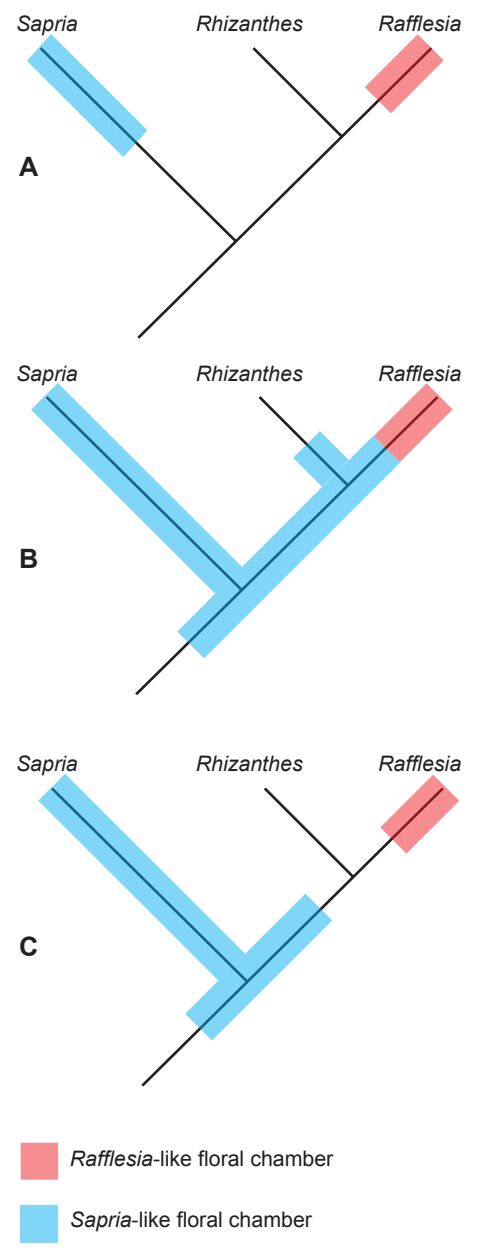
Sapria
Rhizanthes
Rafflesia
A
Sapria
Rhizanthes
Rafflesia
B
Sapria
Rhizanthes
Rafflesia
C
Rafflesia-like floral chamber
Sapria-like floral chamber